Dynamic Response of a Fluid-Loaded Plate Containing Periodic Masses

Andrew J. Hull
Autonomous Systems and Technology Department

NAVSEA
WARFARE CENTERS
NEWPORT

Naval Undersea Warfare Center Division
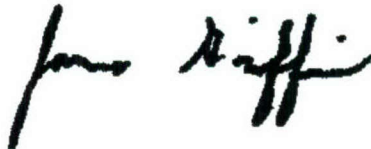# Newport, Rhode Island

PREFACE

This work was performed under Project N00014-04-WX-2-0567, "Simplified Structural Acoustic Model for Active Sonar," principal investigator Andrew J. Hull (Code 8212). The sponsoring activity is the Office of Naval Research, program manager David Drumheller (ONR 333).

The technical reviewer for this report was Benjamin A. Cray (Code 821).

Reviewed and Approved: 31 March 2005

James S. Griffin
Head (*acting*), Autonomous Systems and
Technology Department

REPORT DOCUMENTATION PAGE

1. AGENCY USE ONLY (Leave blank)	2. REPORT DATE 31 March 2005	3. REPORT TYPE AND DATES COVERED

4. TITLE AND SUBTITLE

Dynamic Response of a Fluid-Loaded Plate Containing Periodic Masses

5. FUNDING NUMBERS

PR A821085

6. AUTHOR(S)

Andrew J. Hull

7. PERFORMING ORGANIZATION NAME(S) AND ADDRESS(ES)

Naval Undersea Warfare Center Division
1176 Howell Street
Newport, RI 02841-1708

8. PERFORMING ORGANIZATION REPORT NUMBER

TR 11,662

9. SPONSORING/MONITORING AGENCY NAME(S) AND ADDRESS(ES)

Office of Naval Research
Ballston Centre Tower One
800 North Quincy Street
Arlington VA 22217-5660

10. SPONSORING/MONITORING AGENCY REPORT NUMBER

11. SUPPLEMENTARY NOTES

12a. DISTRIBUTION/AVAILABILITY STATEMENT

Approved for public release; distribution is unlimited.

12b. DISTRIBUTION CODE

13. ABSTRACT (Maximum 200 words)

This report derives the equations of motion of a fluid-loaded thin plate that contains periodically spaced embedded masses and is insonified by a harmonic plane wave. The thin plate equations of motion are coupled to the fluid and to the embedded masses and analyzed to determine the displacement field in the wavenumber-frequency domain. The masses of the periodic discontinuities are then varied to study their influence on the system dynamics. The formulation is then expanded to Timoshenko-Mindlin equations of motion, so that additional plate dynamics can be exhibited and understood. The problem is then posed using thick plate theory and the finite-element method to generate numerical solutions. Finally, thick plate equations of motion that contain bottom attached masses are formulated and presented.

14. SUBJECT TERMS

Plate Theory	Elasticity Theory	Timoshenko-Mindlin Plate Theory
Equations of Motion	Equations of Elasticity	

15. NUMBER OF PAGES
52

16. PRICE CODE

17. SECURITY CLASSIFICATION OF REPORT	18. SECURITY CLASSIFICATION OF THIS PAGE	19. SECURITY CLASSIFICATION OF ABSTRACT	20. LIMITATION OF ABSTRACT
Unclassified	Unclassified	Unclassified	SAR

TABLE OF CONTENTS

LIST OF ILLUSTRATIONS

LIST OF ILLUSTRATIONS (Cont'd)

Figure   **Page**

DYNAMIC RESPONSE OF A FLUID-LOADED PLATE CONTAINING PERIODIC MASSES

1. INTRODUCTION

Plate theory has been analyzed for many years. Thin plate theory[1] is a simplified model that does not incorporate rotary inertia, shear effects, or other plate dynamics. In contrast, thick plate theory[2] usually incorporates all of the dynamics of the plate and is normally used when the plate thickness is on the order of a wavelength of propagating flexural waves within the plate. More thorough investigations have analyzed the propagation of waves (dispersion curves) for the plate without fluid loading,[3] and for the plate in contact with a continuous fluid on one or both sides.[4-6] Recently, closed-form solutions to the equations of motion were derived for an infinite thick plate coupled on one or both sides with fluid loading as it is excited with a continuous forcing function.[7] These previous studies[1-7] provided a thorough basis for understanding plate theory; however, they did not take into account the addition of attached structural components.

The inclusion of periodic mass or stiffness elements in structures has been used for years as a method to obtain the desired static and dynamic response of a system. Numerous investigations of this system have been undertaken to determine the farfield acoustic radiation pattern.[8-10] Throughout the past studies, a model was loaded with a line or point source and the resulting acoustic field was predicted. The problem that has largely been ignored is the displacement field of a thick plate containing periodic masses or stiffeners when it is excited by an incoming acoustic plane wave. In a thin or thick plate with embedded masses, the displacement and stress fields are subjected to different forces than they would otherwise encounter in a homogeneous plate.

This report derives the equations of motion of a fluid-loaded thin plate that contains embedded masses when it is forced by an acoustic plane wave at a specific wavenumber. The thin plate equations of motion are coupled to the fluid and masses and then manipulated to determine the displacement field. This method is then expanded to Timoshenko-Mindlin equations of motion, as well as to thick plate theory using finite-element solutions. Finally, the thick plate equations of motion containing bottom attached masses are formulated and the resultant problem is discussed.

2. PLATE MODELS WITHOUT MASSES

To facilitate a basic understanding of the effects of periodic masses, it is first desirable to list the thin and thick plate theories without the masses and graphically compare the solutions of each plate model in the wavenumber-frequency domain. The three plate models listed in this section have all been previously derived; therefore, only the governing partial differential equations and the final solutions are shown here. They correspond to a thin plate, a thin plate that incorporates shear and rotary inertia effects (i.e., the Timoshenko-Mindlin plate), and a thick plate. A diagram of the modeled system is shown in figure 1. Note that using the coordinate system in the orientation shown in figure 1 results in a negative value of a; the thickness h is a positive value.
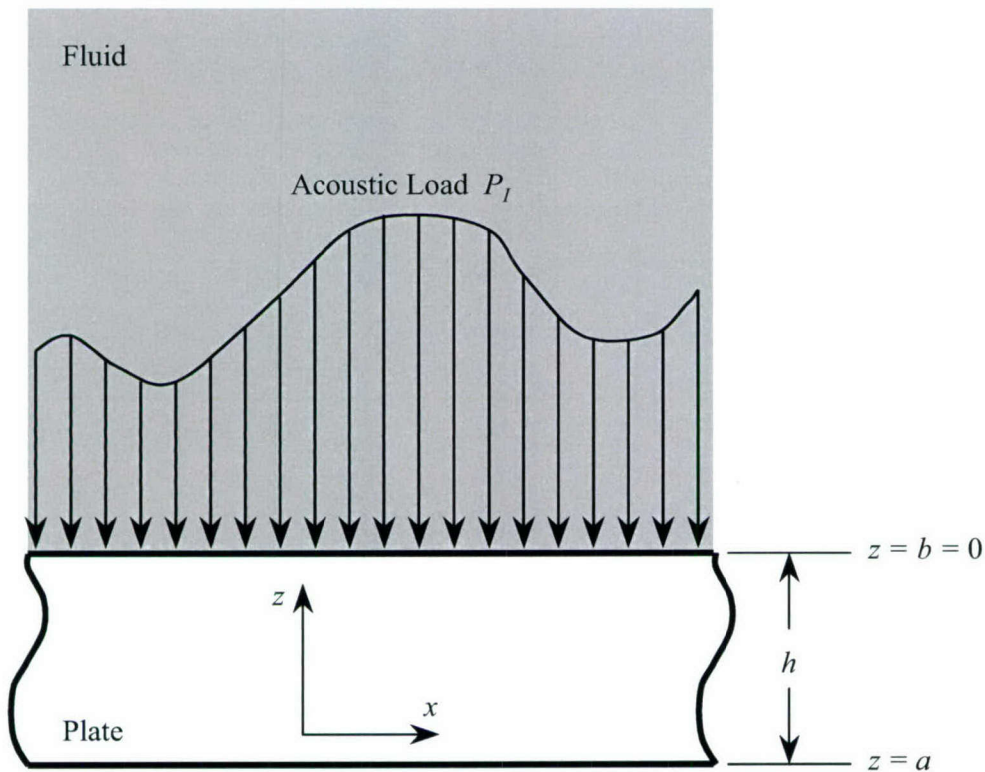
Figure 1. Plate Without Masses Subjected to a Fluid Load

2.1. THIN PLATE WITHOUT MASSES

The first model investigated is that of a thin plate with a fluid load on top. The equation of motion of the thin plate is[11]

$$D\frac{\partial^4 u_z(x,t)}{\partial x^4} + \rho h\frac{\partial^2 u_z(x,t)}{\partial t^2} = -p(x,t) \ , \tag{1}$$

where $u_z(x,t)$ is the displacement of the plate in the z-direction, x is the spatial position, t is time, ρ is the density of the plate, $p(x,t)$ is the applied pressure in the fluid load, and D is the bending stress expressed as

$$D = \frac{Eh^3}{12(1-\upsilon^2)} \ , \tag{2}$$

where E is Young's modulus of the plate and υ is Poisson's ratio of the plate. The acoustic pressure in the fluid is governed by the wave equation and is written as

$$\frac{\partial^2 p(x,z,t)}{\partial z^2} + \frac{\partial^2 p(x,z,t)}{\partial x^2} - \frac{1}{c_f^2}\frac{\partial^2 p(x,z,t)}{\partial t^2} = 0 \ , \tag{3}$$

where $p(x,z,t)$ is the pressure in the fluid and c_f is the compressional wavespeed in the fluid. The interface at the fluid and solid surface of the plate at $z = b$ satisfies the linear momentum equation and is written as

$$\rho_f\frac{\partial^2 u_z(x,b,t)}{\partial t^2} = -\frac{\partial p(x,b,t)}{\partial z} \ , \tag{4}$$

where ρ_f is the density of the fluid. Assuming harmonic response and loading in space and time, equations (1), (3), and (4) can be combined. The resulting expression is the displacement in the z-direction divided by the incident pressure P_I and is written as

$$\frac{U_z(k_x,\omega)}{P_I} = \frac{-2}{Dk_x^4 + \left(\dfrac{\rho_f}{i\gamma} - \rho h\right)\omega^2} \ , \tag{5}$$

4

where k_x is the wavenumber with respect to the x-axis, ω is frequency, and γ is the acoustic wavenumber written as

$$\gamma = \sqrt{\left(\frac{\omega}{c_f}\right)^2 - k_x^2} \ . \tag{6}$$

2.2. TIMOSHENKO-MINDLIN PLATE WITHOUT MASSES

The second model investigated is that of a thin plate that includes the effects of rotary inertia and transverse shear, generally called a Timoshenko-Mindlin plate. This plate is also in contact with a fluid load on top. The equation of motion for this plate is[12]

$$D\frac{\partial^4 u_z(x,t)}{\partial x^4} - \left(\frac{D\rho}{\kappa G} + \frac{\rho h^3}{12}\right)\frac{\partial^4 u_z(x,t)}{\partial x^2 \partial t^2} + \left(\frac{\rho^2 h^3}{12\kappa G}\right)\frac{\partial^4 u_z(x,t)}{\partial t^4} + \rho h\frac{\partial^2 u_z(x,t)}{\partial t^2}$$
$$= -p(x,t) + \left(\frac{D}{\kappa Gh}\right)\frac{\partial^2 p(x,t)}{\partial x^2} - \left(\frac{\rho h^2}{12\kappa G}\right)\frac{\partial^2 p(x,t)}{\partial t^2}, \tag{7}$$

where G is the shear modulus of the plate and κ is the shear coefficient of the plate, typically computed for a rectangular section using

$$\kappa = \frac{5}{6 - \upsilon} \ . \tag{8}$$

Assuming harmonic responses in space and time, equations (3), (4), and (7) can be combined. The resulting expression is the displacement in the z-direction divided by the incident pressure and is written as

$$\frac{U_z(k_x,\omega)}{P_I} = \frac{-2 - \left(\frac{2D}{\kappa Gh}\right)k_x^2 + \left(\frac{2\rho h^2}{12\kappa G}\right)\omega^2}{Dk_x^4 + \left(\frac{D\rho_f}{i\gamma\kappa Gh} - \frac{D\rho}{\kappa G} - \frac{\rho h^3}{12}\right)\omega^2 k_x^2 + \left(\frac{\rho^2 h^3}{12\kappa G} - \frac{\rho_f \rho h^2}{12i\gamma\kappa G}\right)\omega^4 + \left(\frac{\rho_f}{i\gamma} - \rho h\right)\omega^2} . \tag{9}$$

5

2.3. THICK PLATE WITHOUT MASSES

The third model investigated is that of a thick plate—this model is sometimes referred to as the exact or complete solution. The equation of motion for a three-dimensional medium is[13]

$$\mu\nabla^2\mathbf{u} + (\lambda + \mu)\nabla\nabla\bullet\mathbf{u} = \rho\frac{\partial^2\mathbf{u}}{\partial t^2} , \qquad (10)$$

where λ and μ are the Lamé constants, $\bullet$ denotes a vector dot product; and $\mathbf{u}$ is the Cartesian coordinate displacement vector of the plate. Assuming harmonic response in space and time, equations (3), (4), and (10) can be combined. The resulting expression is the displacement in the z-direction divided by the incident pressure and is written as[7]

$$\frac{U_z(k_x,z,\omega)}{P_I} = \frac{U_z^{Ts}(k_x,z,\omega)}{\mu\Delta_s(k_x,\omega)} , \qquad (11)$$

where z is the spatial location (in meters), and

$$\begin{aligned}
U_z^{Ts}(k_x,z,\omega) = & f_1\{\sin(\alpha z) - \cos(\beta h)\sin[\alpha(z+h)]\} \\
& + f_2\{\sin(\beta z) - \cos(\alpha h)\sin[\beta(z+h)]\} \\
& + f_3\sin(\alpha h)\cos[\beta(z+h)] + f_4\sin(\beta h)\cos[\alpha(z+h)],
\end{aligned} \qquad (12)$$

and

$$\begin{aligned}
\Delta_s(k_x,\omega) = & f_5(k_x,\omega)\cos(\alpha h)\cos(\beta h) + f_6(k_x,\omega)\cos(\alpha h)\sin(\beta h) \\
& + f_7(k_x,\omega)\sin(\alpha h)\cos(\beta h) + f_8(k_x,\omega)\sin(\alpha h)\sin(\beta h) - f_5(k_x,\omega).
\end{aligned} \qquad (13)$$

The constants in equations (12) and (13) are

$$f_1(k_x,\omega) = -8\alpha^2\beta k_x^2(\beta^2 - k_x^2) , \qquad (14)$$

$$f_2(k_x,\omega) = -4\alpha k_x^2(\beta^2 - k_x^2)^2 , \qquad (15)$$

$$f_3(k_x, \omega) = 16\alpha^2 \beta k_x^4 , \tag{16}$$

$$f_4(k_x, \omega) = 2\alpha(\beta^2 - k_x^2)^3 , \tag{17}$$

$$f_5(k_x, \omega) = -8\alpha\beta k_x^2(\beta^2 - k_x^2)^2 , \tag{18}$$

$$f_6(k_x, \omega) = i\rho_f(\gamma\rho)^{-1}\alpha(\beta^2 - k_x^2)^2(\beta^2 + k_x^2)^2 , \tag{19}$$

$$f_7(k_x, \omega) = 4i\rho_f(\gamma\rho)^{-1}\alpha^2\beta k_x^2(\beta^2 + k_x^2)^2 , \tag{20}$$

and

$$f_8(k_x, \omega) = (\beta^2 - k_x^2)^4 + 16\alpha^2\beta^2 k_x^4 . \tag{21}$$

In equations (12) through (21), α is the modified wavenumber associated with the dilatational wave and is expressed as

$$\alpha = \sqrt{k_d^2 - k_x^2} , \tag{22}$$

where k_d is the dilatational wavenumber and is equal to ω/c_d, with c_d being the dilatational wavespeed (m/s); and β is the modified wavenumber (rad/m) associated with the shear wave and is expressed as

$$\beta = \sqrt{k_s^2 - k_x^2} , \tag{23}$$

where k_s is the shear wavenumber (rad/m) and is equal to ω/c_s, with c_s being the shear wavespeed (m/s). The relationships between wavespeeds c_d and c_s and the plate's Lamé constants λ and μ are determined by

$$c_d = \sqrt{\frac{\lambda + 2\mu}{\rho}} , \tag{24}$$

7

and

$$c_s = \sqrt{\frac{\mu}{\rho}}.$$ (25)

Finally, the relationships between the Lamé constants and Young's modulus, shear modulus, and Poisson's ratio are given by

$$\lambda = \frac{E\upsilon}{(1+\upsilon)(1-2\upsilon)}$$ (26)

and

$$\mu = G = \frac{E}{2(1+\upsilon)}.$$ (27)

2.4. COMPARISON OF MODELS WITHOUT MASSES

The models without masses are now compared using a numerical example. The properties of the plate and fluid are listed in table 1. The results are displayed graphically as magnitude of normalized velocity divided by incident pressure (a dimensionless quantity) versus wavenumber. This expression is determined by

$$\frac{V_z^n(k_x,\omega)}{P_I} = i\omega\rho_f c_f \frac{U_z(k_x,\omega)}{P_I}.$$ (28)

Figure 2 is an image of thin plate normalized velocity versus wavenumber and frequency and was generated using equations (5) and (28). Figure 3 is an image of thin plate (with rotary inertia and shear effects) normalized velocity versus wavenumber and frequency and was generated using equations (9) and (28). Figure 4 is an image of thick plate normalized velocity versus wavenumber and frequency and was generated using equations (11) and (28). Figures 5 through 24 are constant frequency cuts of figures 2, 3, and 4 overlaid for a frequency range of 500 Hz to 10 kHz in 500-Hz increments. In figures 2 through 24, the velocity is displayed on a decibel scale. Note that the thin plate and thick plate solutions begin to diverge at about 1.5 kHz, and the Timoshenko-Mindlin plate and thick plate solutions begin to diverge at about 3.5 kHz.

8

Table 1. Parameters Used for Fluid-Loaded Plate Without Mass

Plate Properties	
Thickness, h	0.04 m
Young's Modulus, E	7.0e8 N/m^2
Shear Modulus, G	2.5e8 N/m^2
Poisson's Ratio, υ	0.4 (dimensionless)
Density, ρ	1200 kg/m^3
Fluid Properties	
Compressional Wavespeed, c_f	1500 m/s
Density, ρ_f	1025 kg/m^3

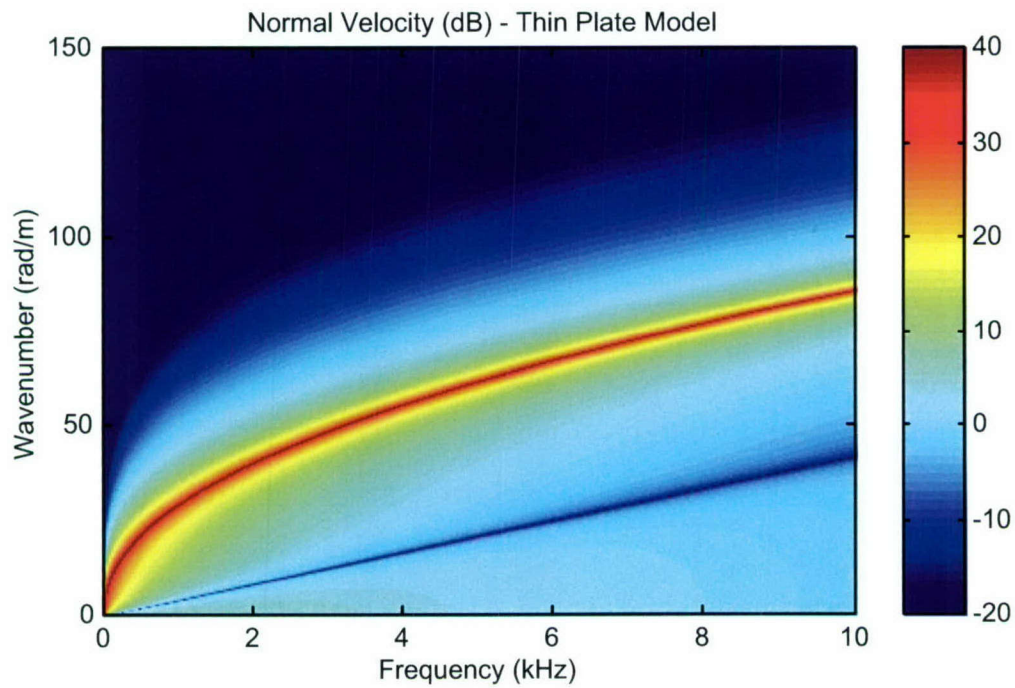*Figure 2. Normalized Velocity Versus Wavenumber and Frequency Without Masses—*
Modeled Using Thin Plate Theory

Normal Velocity (dB) - Timoshenko-Mindlin Plate

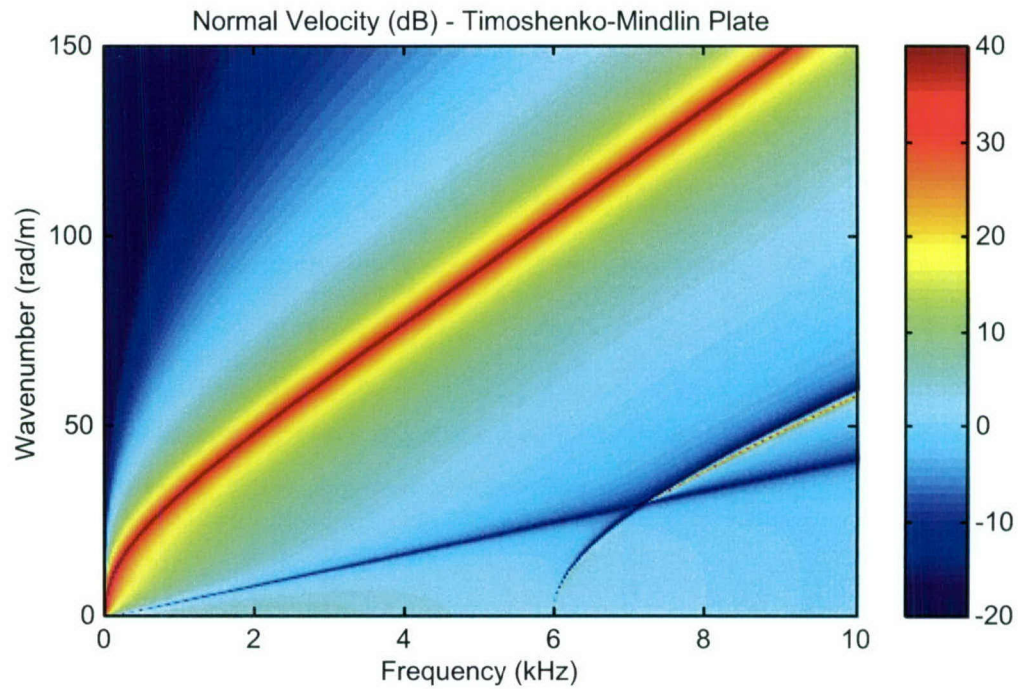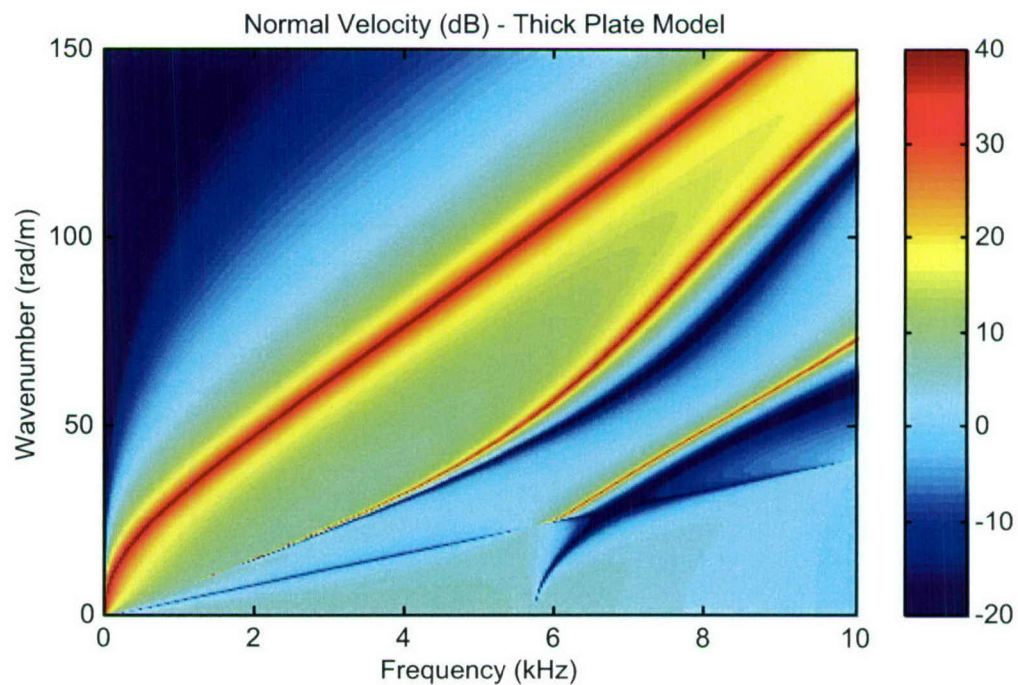*Figure 3. Normalized Velocity Versus Wavenumber and Frequency Without Masses—Modeled Using Timoshenko-Mindlin Plate Theory*

Normal Velocity (dB) - Thick Plate Model

Figure 4. Normalized Velocity Versus Wavenumber and Frequency Without Masses—Modeled Using Thick Plate Theory

Frequency of 500 Hz

Figure 5. Normalized Velocity Versus Wavenumber Without Masses at 500 Hz

Frequency of 1000 Hz

Figure 6. Normalized Velocity Versus Wavenumber Without Masses at 1.0 kHz
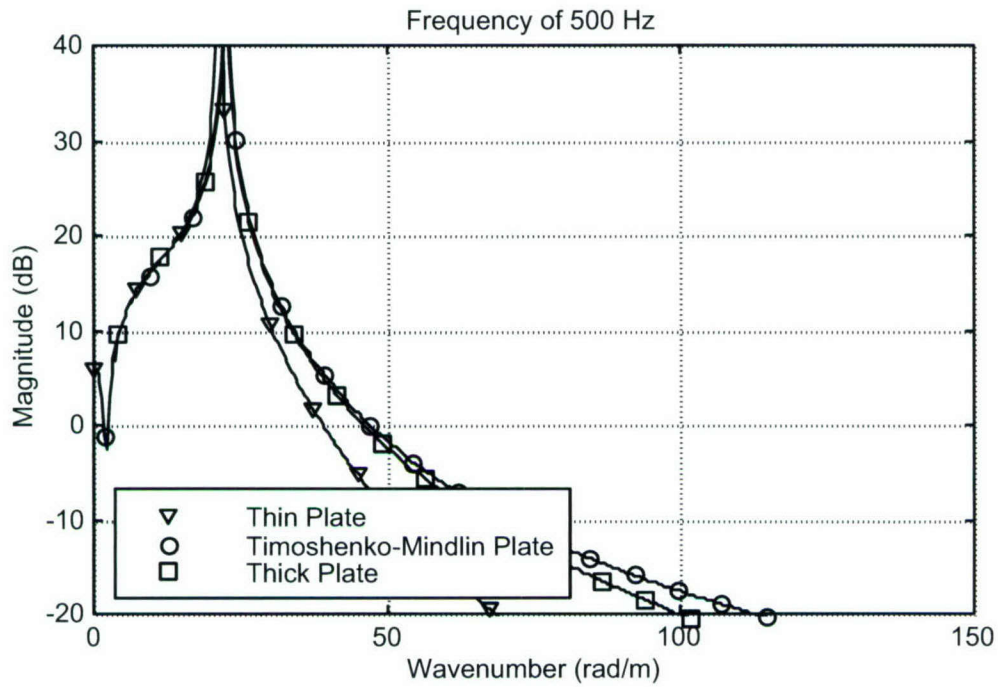
11

Figure 7. Normalized Velocity Versus Wavenumber Without Masses at 1.5 kHz

Figure 8. Normalized Velocity Versus Wavenumber Without Masses at 2.0 kHz

12

Frequency of 2500 Hz

Figure 9. *Normalized Velocity Versus Wavenumber Without Masses at 2.5 kHz*
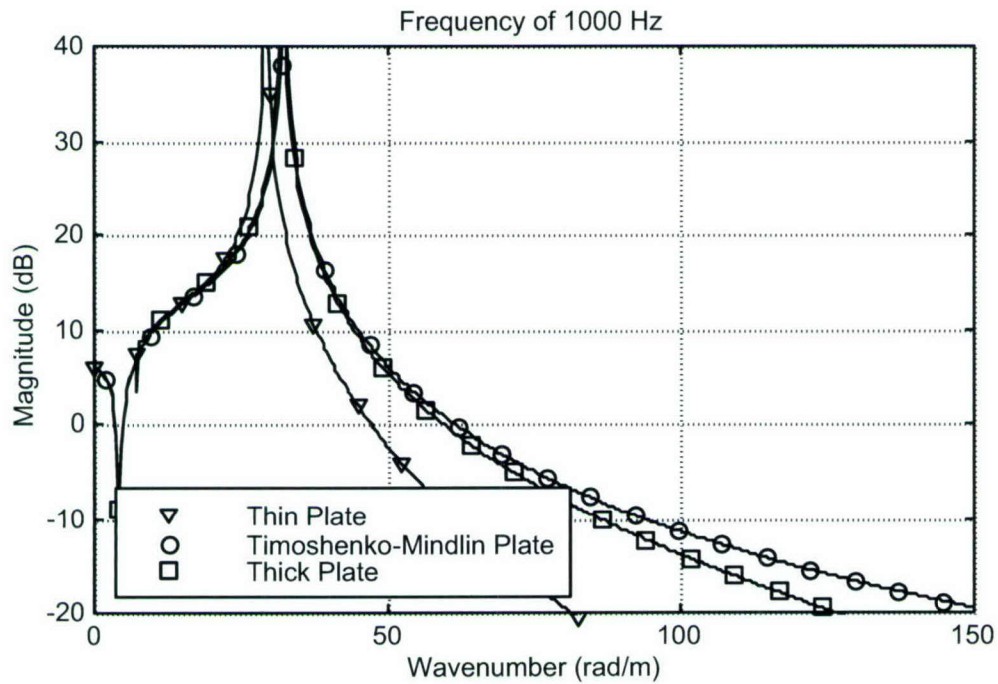
Frequency of 3000 Hz

Figure 10. *Normalized Velocity Versus Wavenumber Without Masses at 3.0 kHz*

13

Figure 11. Normalized Velocity Versus Wavenumber Without Masses at 3.5 kHz

Figure 12. Normalized Velocity Versus Wavenumber Without Masses at 4.0 kHz
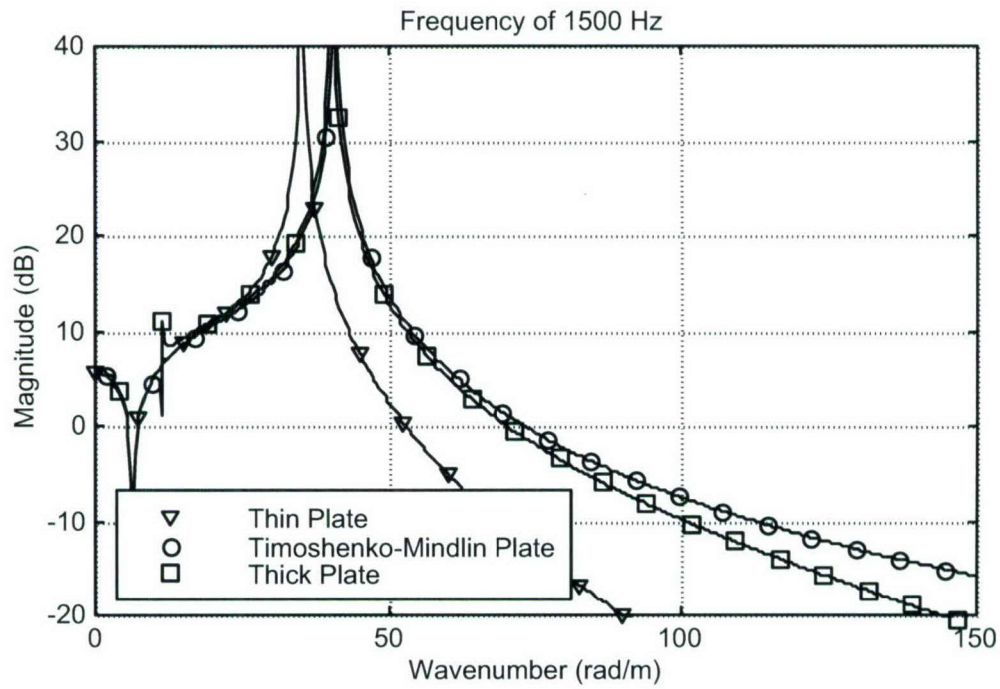
14

Figure 13. Normalized Velocity Versus Wavenumber Without Masses at 4.5 kHz

Figure 14. Normalized Velocity Versus Wavenumber Without Masses at 5.0 kHz

Figure 15. Normalized Velocity Versus Wavenumber Without Masses at 5.5 kHz

Figure 16. Normalized Velocity Versus Wavenumber Without Masses at 6.0 kHz

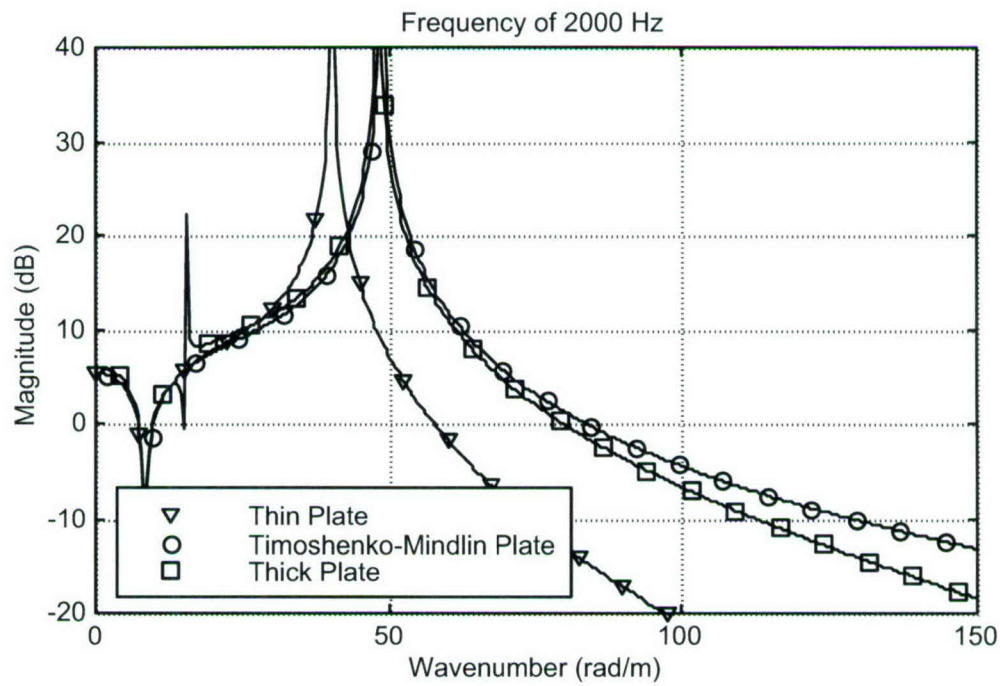*Figure 17. Normalized Velocity Versus Wavenumber Without Masses at 6.5 kHz*
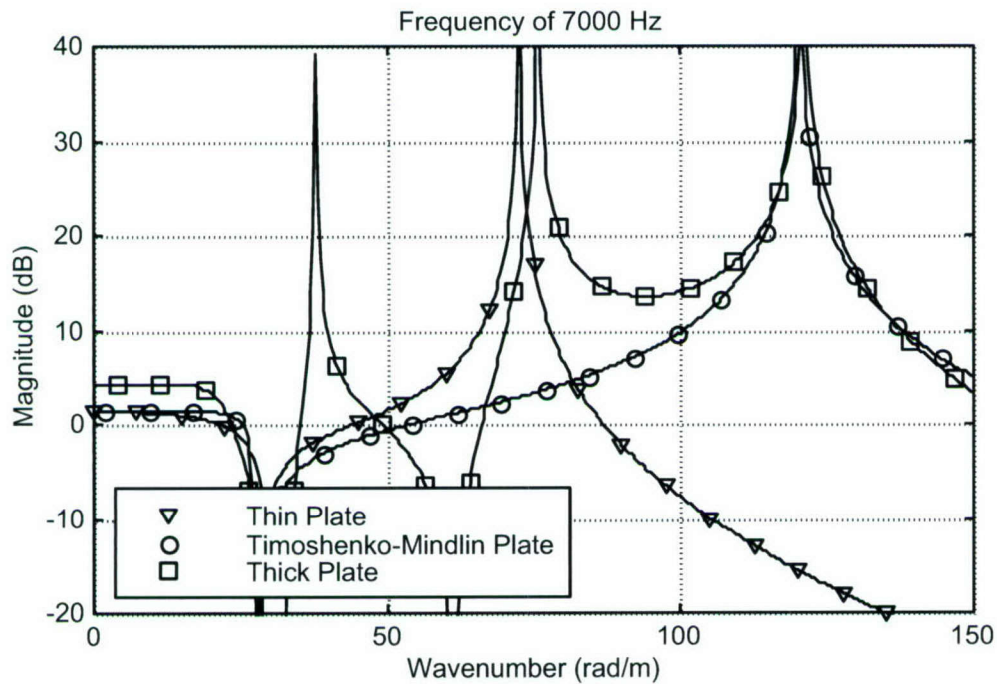
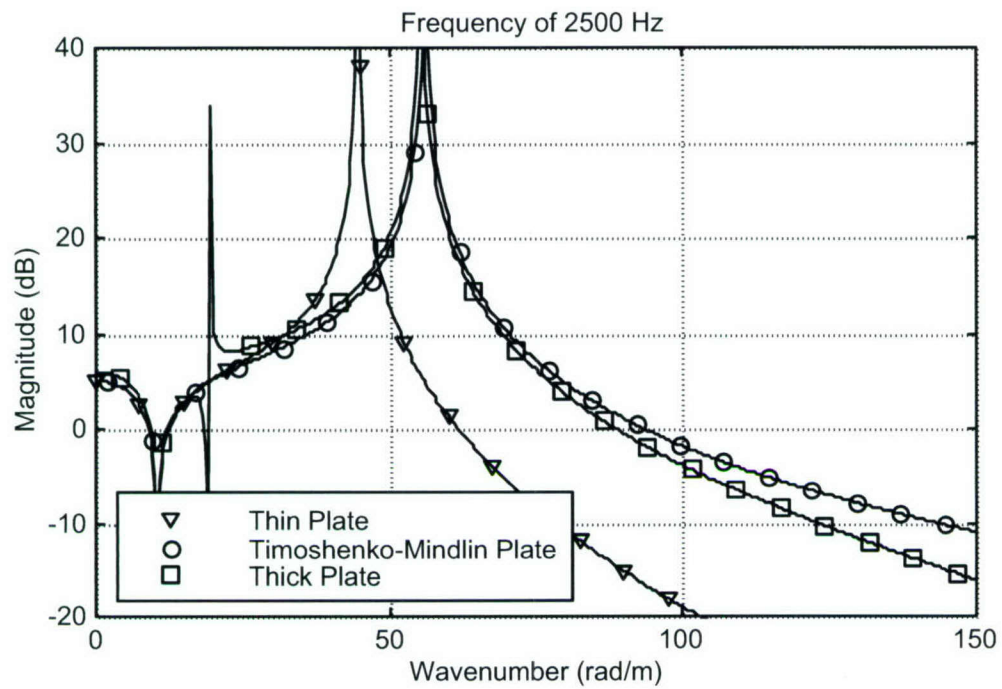*Figure 18. Normalized Velocity Versus Wavenumber Without Masses at 7.0 kHz*
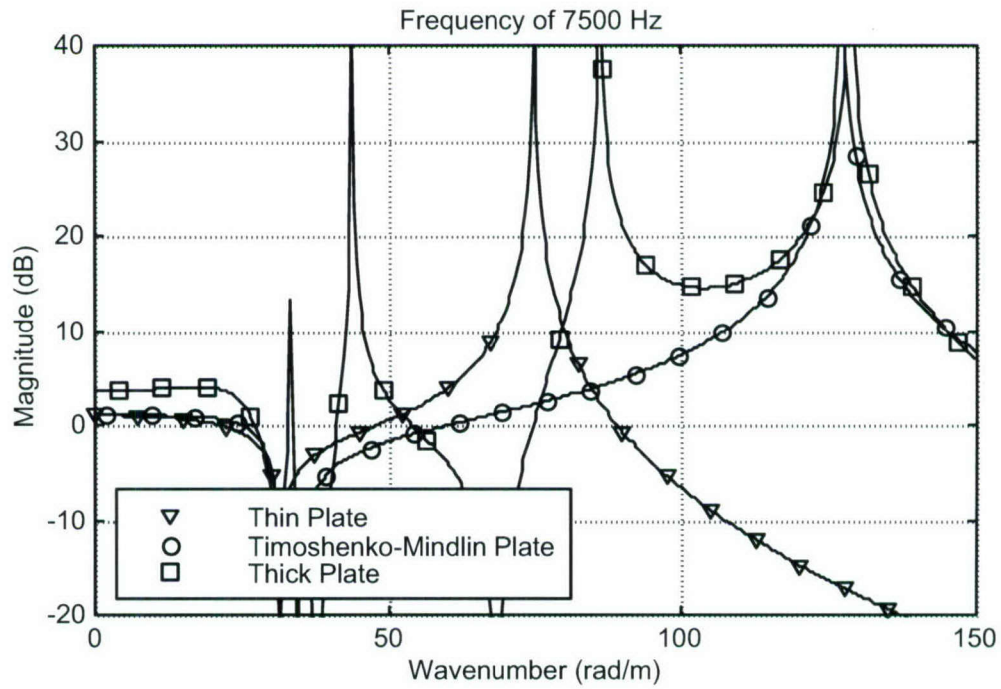
Figure 19. Normalized Velocity Versus Wavenumber Without Masses at 7.5 kHz
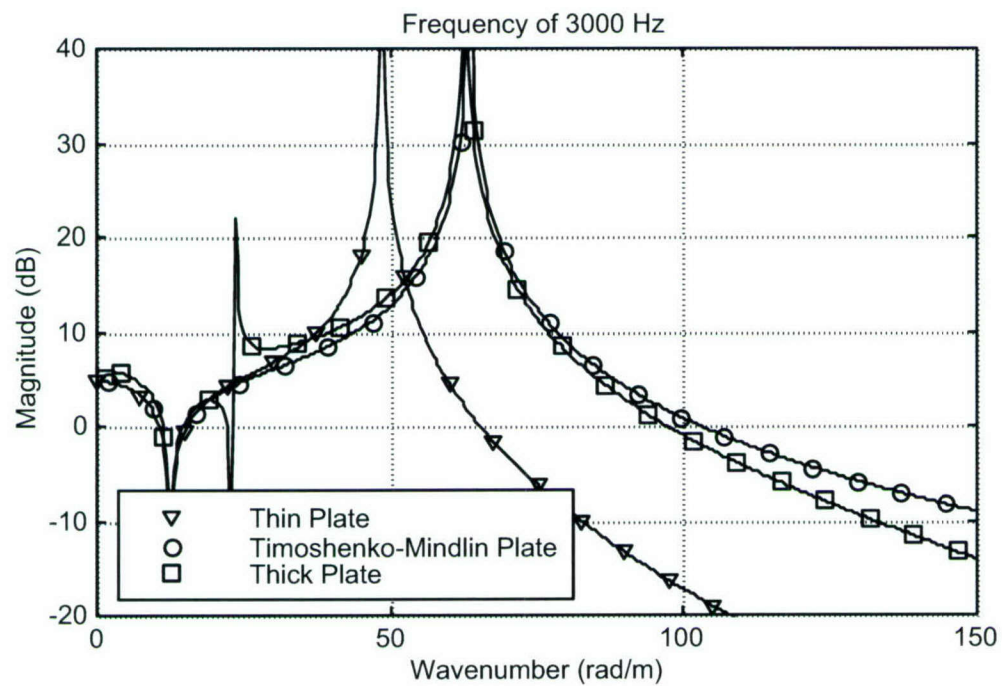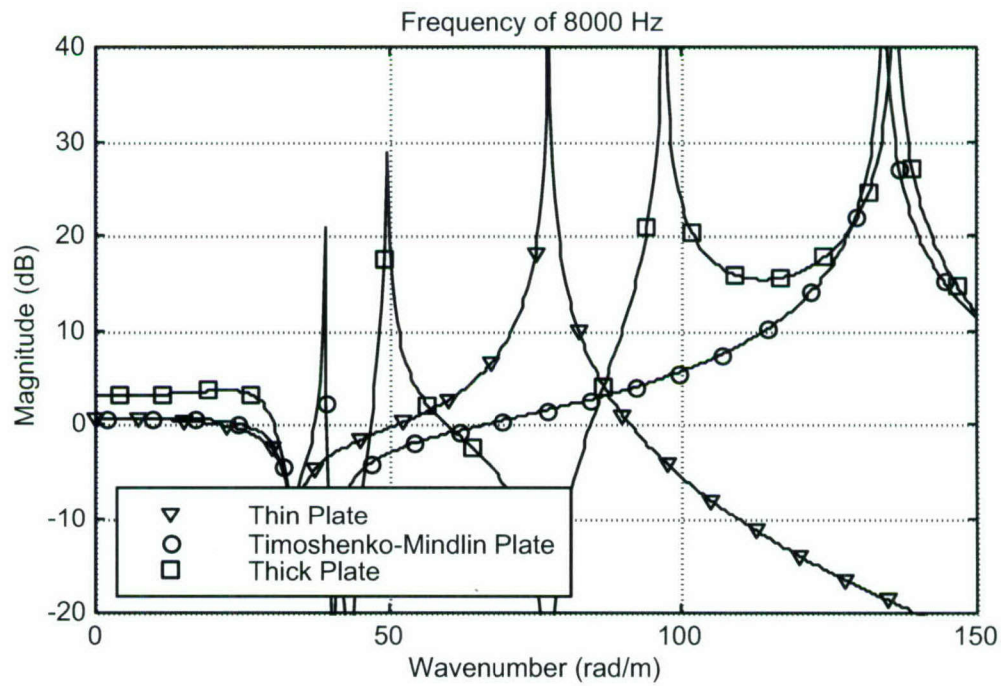

Figure 20. Normalized Velocity Versus Wavenumber Without Masses at 8.0 kHz
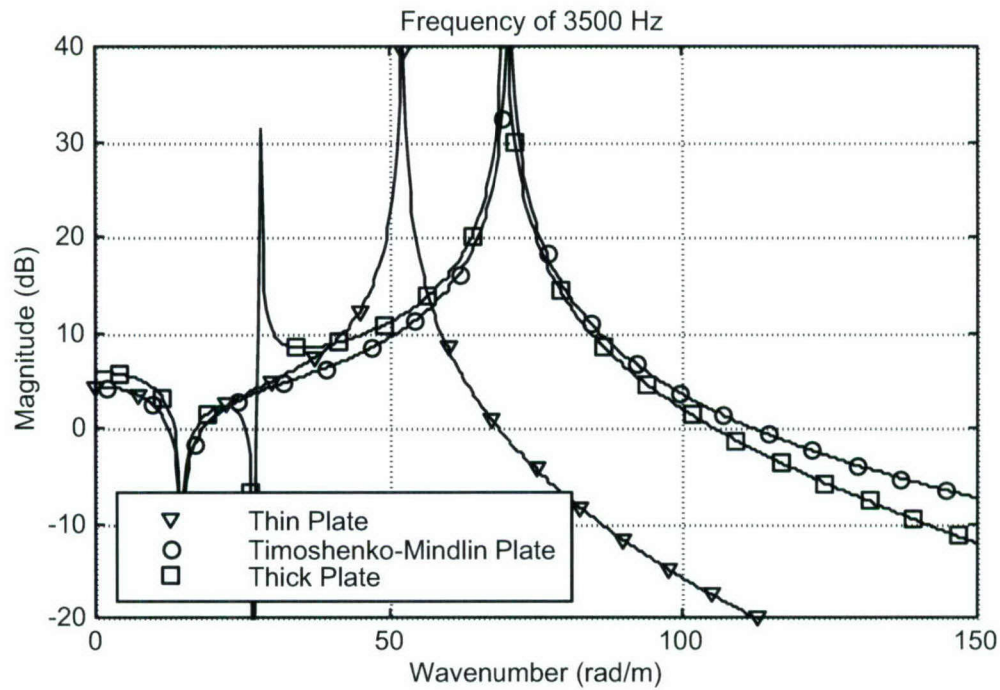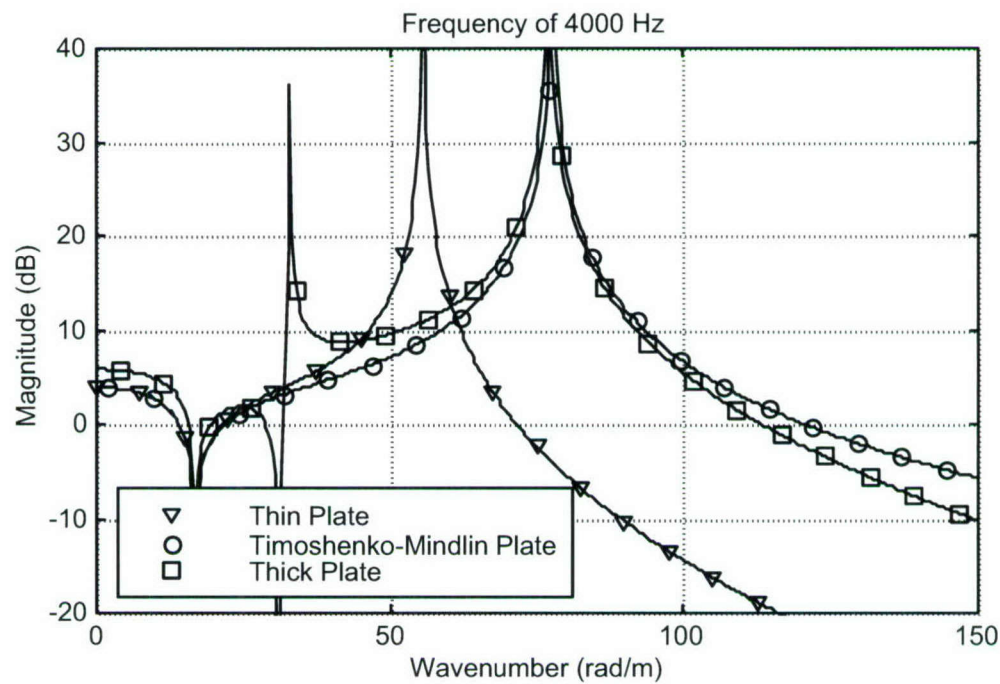
18
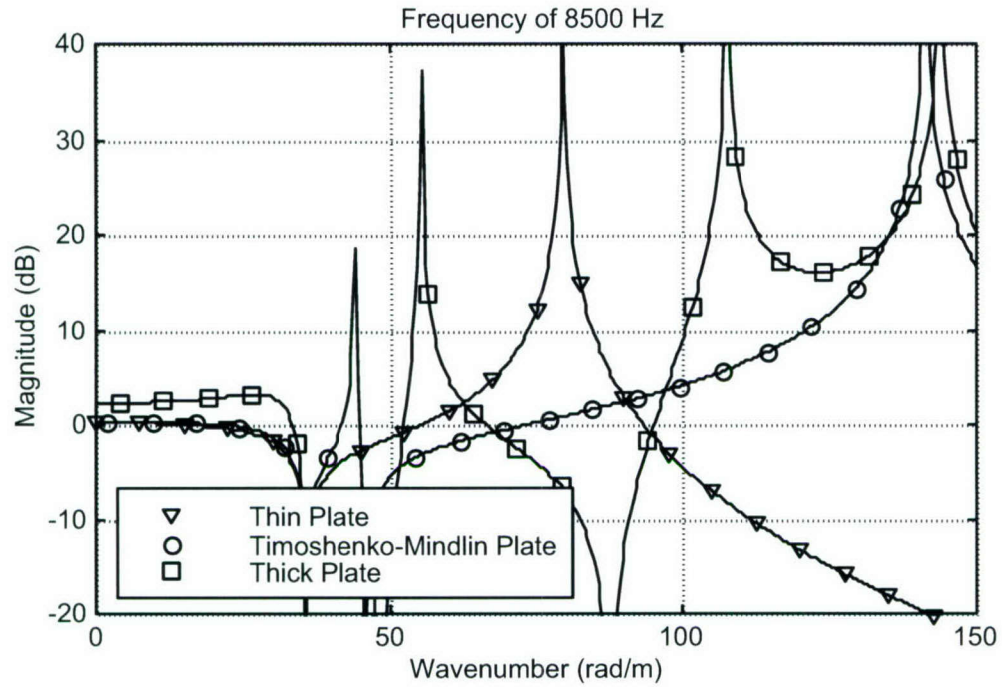
Figure 21. Normalized Velocity Versus Wavenumber Without Masses at 8.5 kHz
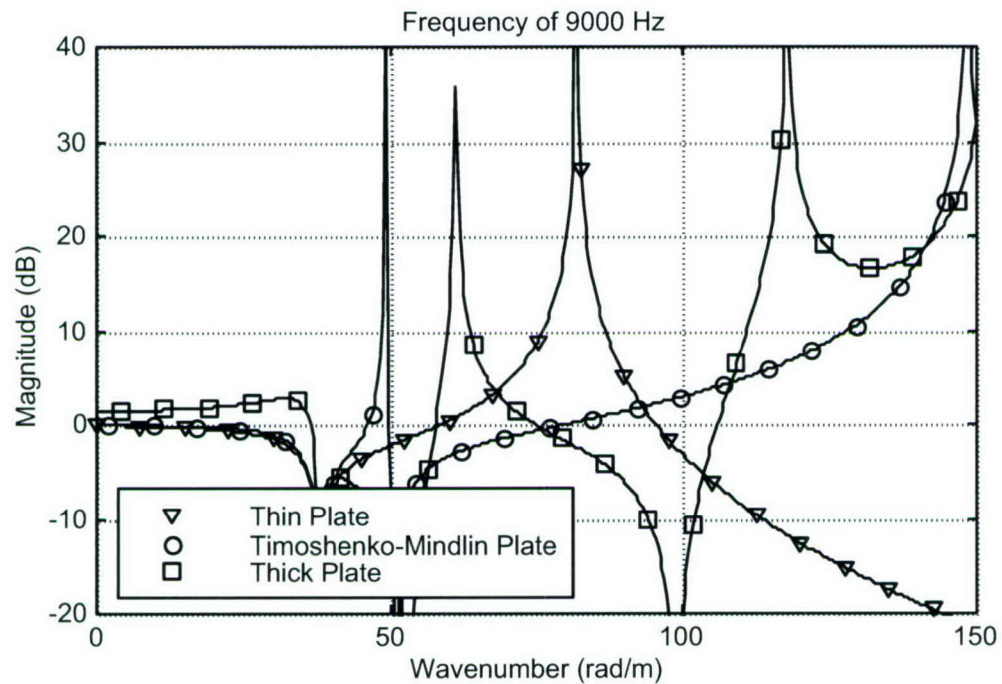
Figure 22. Normalized Velocity Versus Wavenumber Without Masses at 9. 0 kHz
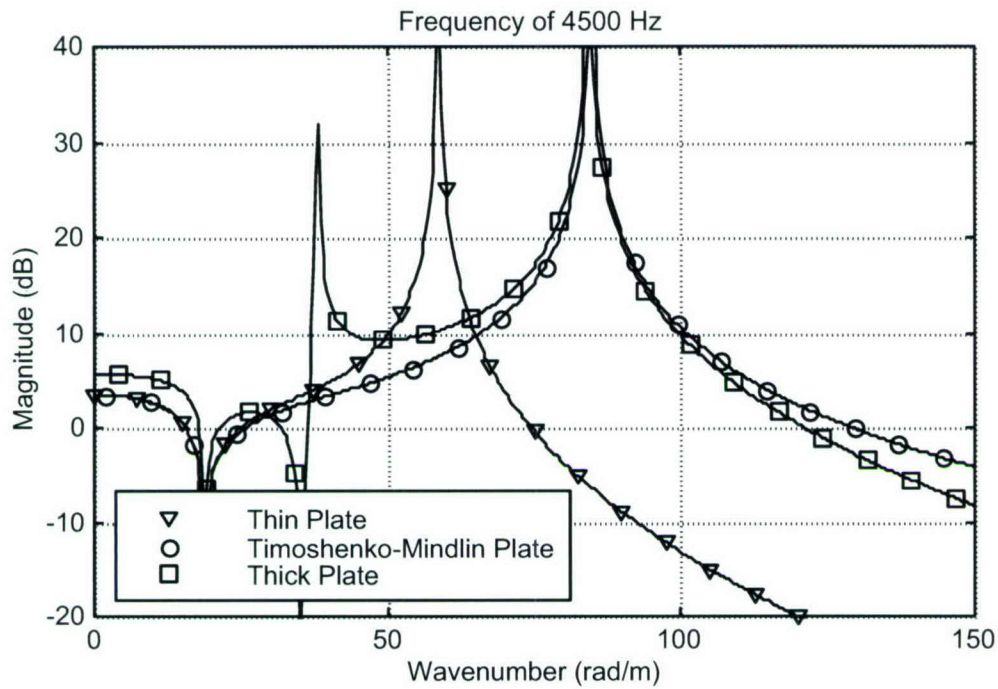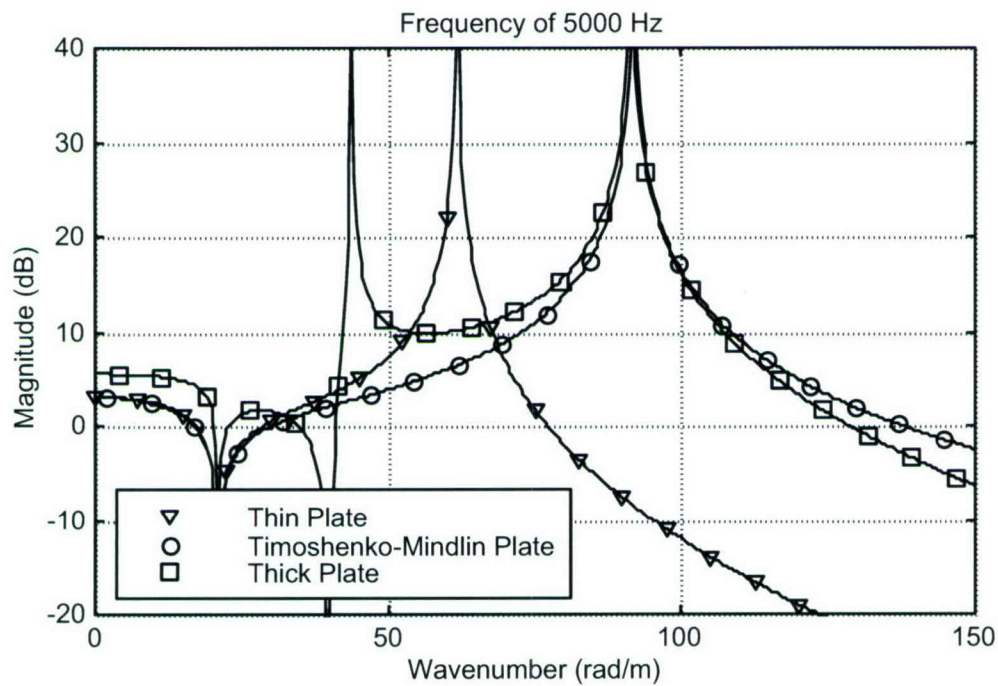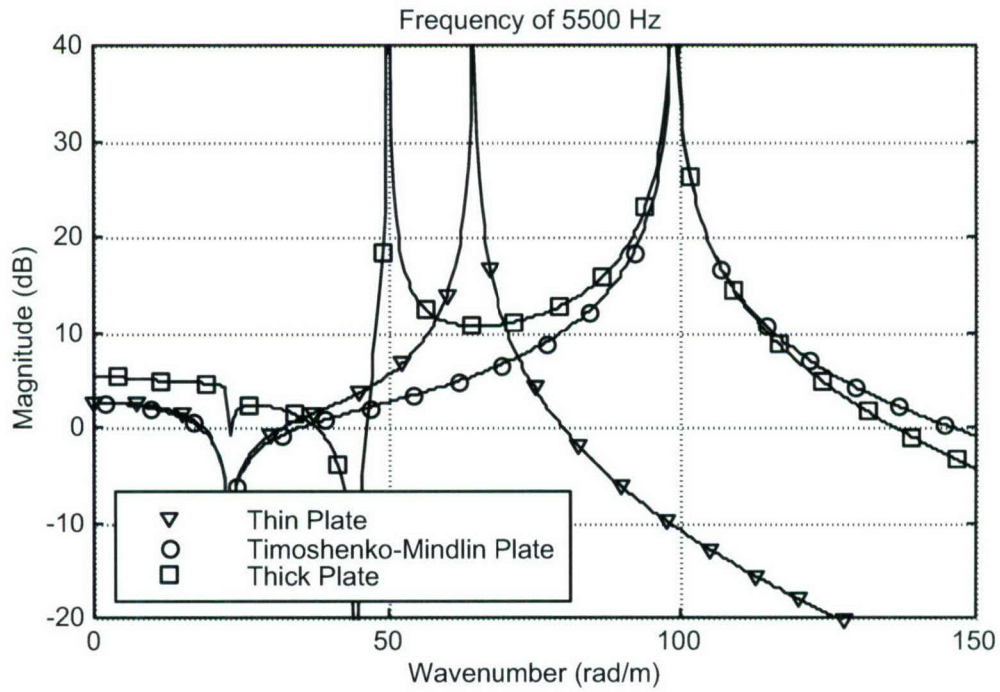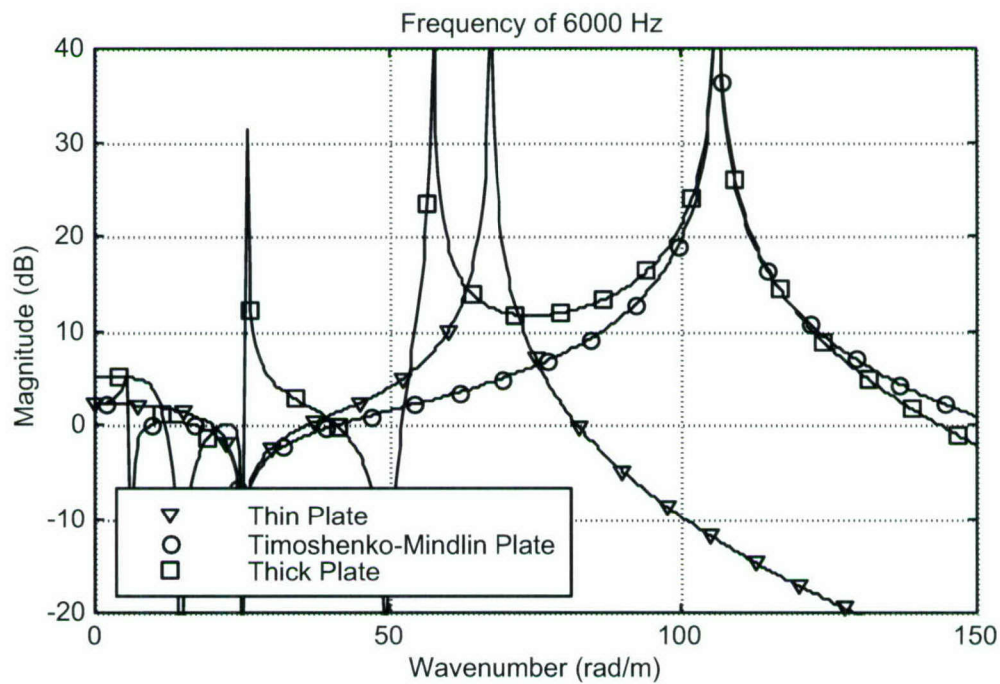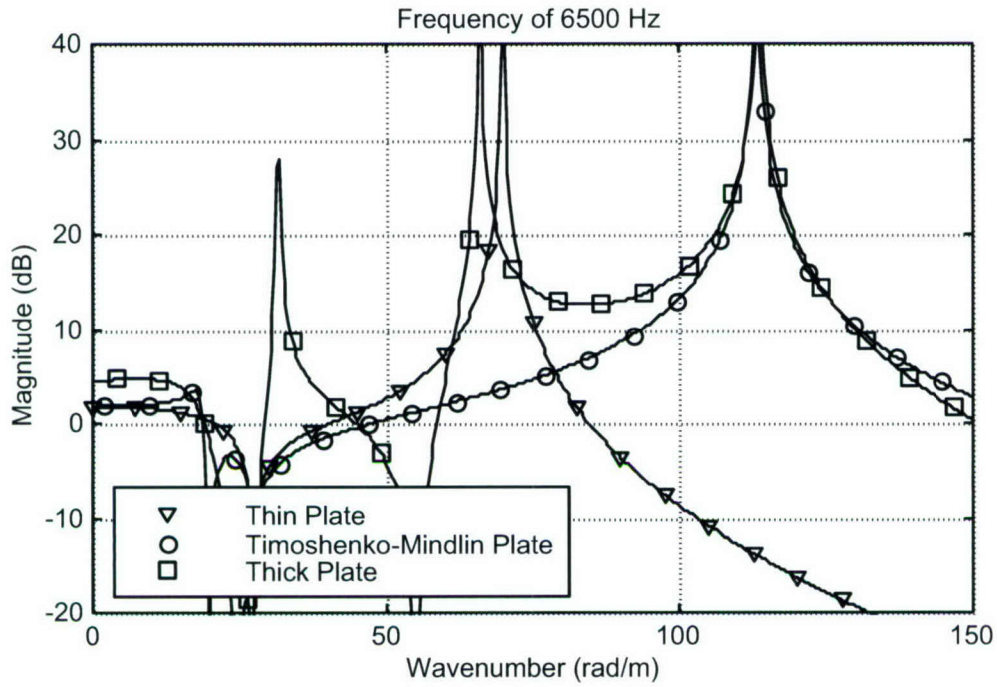
19

Frequency of 9500 Hz
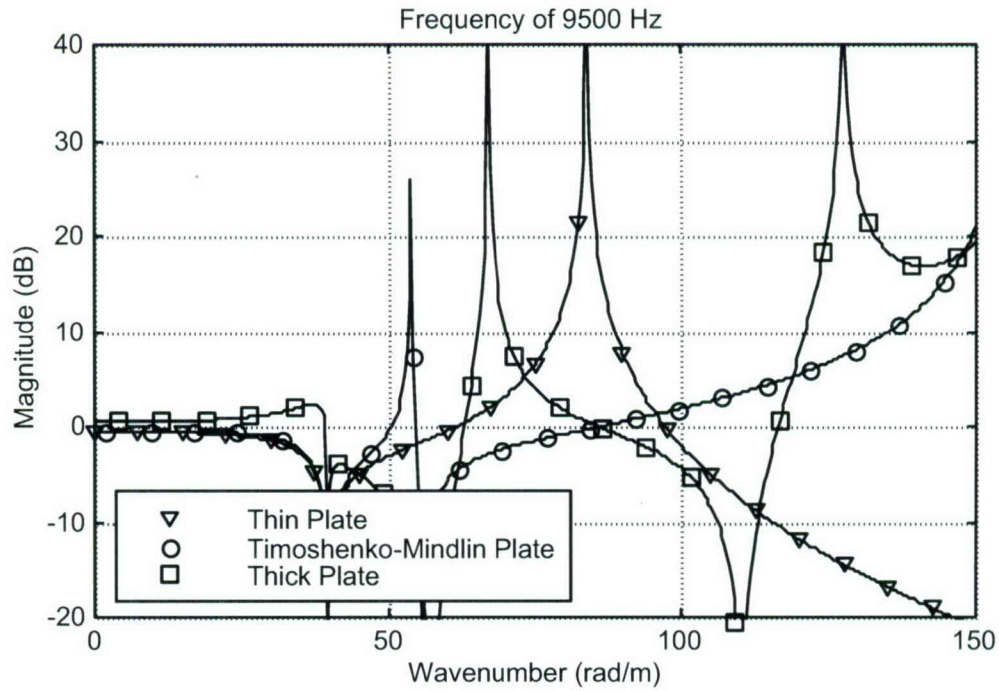
Figure 23. Normalized Velocity Versus Wavenumber Without Masses at 9.5 kHz

Frequency of 10000 Hz
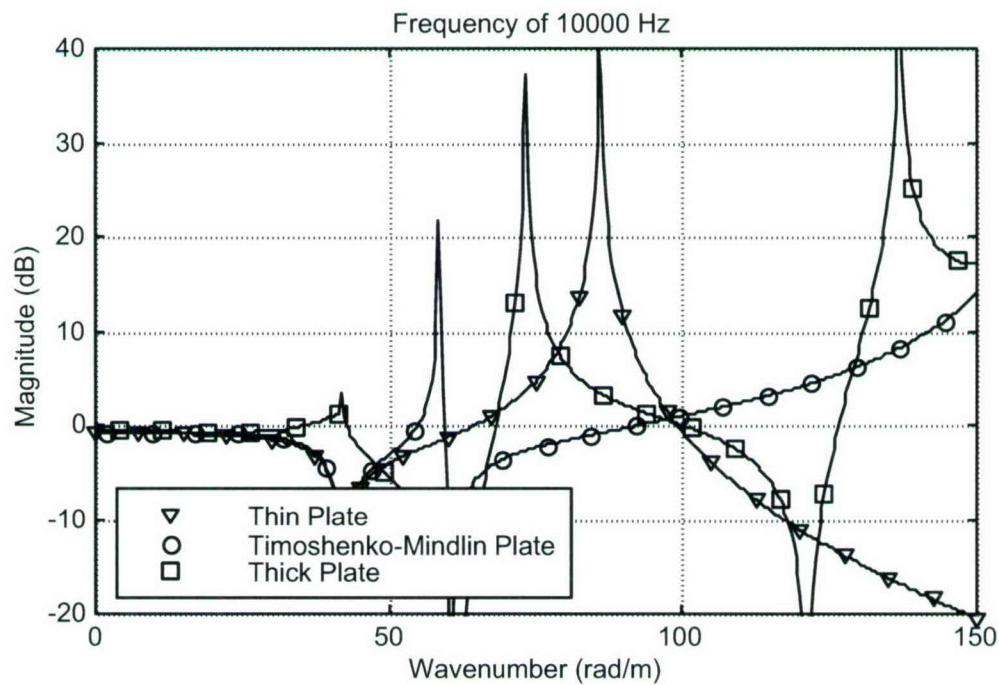
Figure 24. Normalized Velocity Versus Wavenumber Without Masses at 10.0 kHz

3. PLATE MODELS WITH PERIODIC MASSES

The three plate models (thin plate, Timoshenko-Mindlin plate, and thick plate) are now modified to account for periodic masses, which act as applied forces; see the right-hand side of equations (1), (7), and (10). A diagram of the modeled system is shown in figure 25.
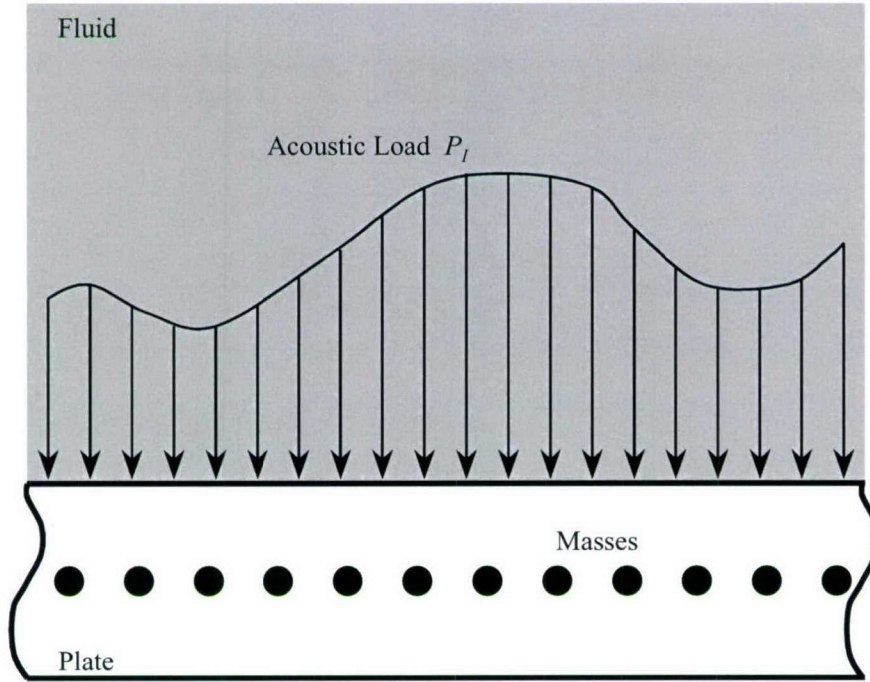
Figure 25. Plate with Masses Subjected to a Fluid Load

3.1. THIN PLATE WITH MASSES

The first model investigated is that of a thin plate containing the periodic masses with a fluid load acting on the upper surface of the plate. The equation of motion of the thin plate is

$$D\frac{\partial^4 u_z(x,t)}{\partial x^4} + \rho h\frac{\partial^2 u_z(x,t)}{\partial t^2} = -p(x,t) - p_M(x,t) \ , \tag{29}$$

with

$$p_M(x,t) = \sum_{n=-\infty}^{\infty} M \frac{\partial^2 u_z(x,t)}{\partial t^2} \delta(x-nL) \; , \tag{30}$$

where M is the mass per unit length of the masses, L is the spacing between adjacent masses, and δ is the Dirac delta function. The problem is transformed into the wavenumber-frequency domain using

$$u_z(x,t) = U_z(k_x,\omega) \exp(ik_x x) \exp(i\omega t), \tag{31}$$

$$p(x,t) = P(k_x,\omega) \exp(ik_x x) \exp(i\omega t), \tag{32}$$

and

$$p_M(x,t) = P_M(k_x,\omega) \exp(ik_x x) \exp(i\omega t). \tag{33}$$

Implicit in equations (31) through (33) is that the medium has infinite extent in the x-direction. Inserting equation (32) into equation (3) yields

$$P(k_x,\omega) = G \exp(i\gamma z) + P_I \exp(-i\gamma z). \tag{34}$$

Then, inserting equations (31) and (34) into equation (4) at $z = 0$ gives the expression

$$P(k_x,\omega) = \frac{\omega^2 \rho_f}{i\gamma} U_z(k_x,\omega) + 2P_I. \tag{35}$$

The periodic mass term in equation (30) is transformed by inserting equation (31), applying Poisson's summation formula, and rewriting it as

$$P_M(k_x,\omega) = \frac{-M\omega^2}{L} \sum_{n=-\infty}^{\infty} U_z\!\left(k_x + \frac{2\pi n}{L}\right). \tag{36}$$

Inserting equations (31), (32), (35), and (36) into equation (29) yields

$$\left(Dk_x^4 - \rho h\omega^2 + \frac{\rho_f \omega^2}{i\gamma}\right) U_z(k_x,\omega) = -2P_I + \frac{M\omega^2}{L} \sum_{n=-\infty}^{\infty} U_z\!\left(k_x + \frac{2\pi n}{L}\right). \tag{37}$$

22

Rearranging gives

$$U_z(k_x, \omega) = -2P_I Y(k_x, \omega) + \frac{M\omega^2}{L} \left[\sum_{n=-\infty}^{\infty} U_z\left(k_x + \frac{2\pi n}{L}\right) \right] Y(k_x, \omega), \tag{38}$$

where

$$Y(k_x, \omega) = \frac{1}{Dk_x^4 - \rho h \omega^2 + \dfrac{\rho_f \omega^2}{i\gamma}}. \tag{39}$$

The substitution of

$$k_x \to k_x + \frac{2\pi m}{L} \tag{40}$$

is now applied to equation (38) yielding

$$
\begin{aligned}
U_z\left(k_x + \frac{2\pi m}{L}, \omega\right) = & -2P_I Y\left(k_x + \frac{2\pi m}{L}, \omega\right) \\
& + \frac{M\omega^2}{L} \left[\sum_{n=-\infty}^{\infty} U_z\left(k_x + \frac{2\pi n}{L} + \frac{2\pi m}{L}\right) \right] Y\left(k_x + \frac{2\pi m}{L}, \omega\right).
\end{aligned}
\tag{41}
$$

Taking the infinite summation of equation (41) with respect to m gives

$$
\begin{aligned}
\sum_{m=-\infty}^{\infty} U_z\left(k_x + \frac{2\pi m}{L}, \omega\right) = & -2P_I \sum_{m=-\infty}^{\infty} Y\left(k_x + \frac{2\pi m}{L}, \omega\right) \\
& + \frac{M\omega^2}{L} \sum_{m=-\infty}^{\infty} \left\{ \left[\sum_{n=-\infty}^{\infty} U_z\left(k_x + \frac{2\pi n}{L} + \frac{2\pi m}{L}\right) \right] Y\left(k_x + \frac{2\pi m}{L}, \omega\right) \right\}.
\end{aligned}
\tag{42}
$$

Using the shifting property of infinite summations, the second term on the right-hand side of equation (42) can be changed to

$$\sum_{m=-\infty}^{\infty} \left[\sum_{n=-\infty}^{\infty} U_z\left(k_x + \frac{2\pi n}{L} + \frac{2\pi m}{L}\right) \right] Y(k_x + \frac{2\pi m}{L}, \omega)$$

$$= \sum_{n=-\infty}^{\infty} U_z\left(k_x + \frac{2\pi n}{L}\right) \sum_{m=-\infty}^{\infty} Y(k_x + \frac{2\pi m}{L}, \omega). \tag{43}$$

Inserting equation (43) into equation (42) yields

$$\sum_{m=-\infty}^{\infty} U_z(k_x + \frac{2\pi m}{L}, \omega) = -2P_I \sum_{m=-\infty}^{\infty} Y(k_x + \frac{2\pi m}{L}, \omega)$$

$$+ \frac{M\omega^2}{L} \sum_{n=-\infty}^{\infty} U_z\left(k_x + \frac{2\pi n}{L}\right) \sum_{m=-\infty}^{\infty} Y(k_x + \frac{2\pi m}{L}, \omega). \tag{44}$$

Solving for the summated displacement term yields

$$\sum_{n=-\infty}^{\infty} U_z(k_x + \frac{2\pi n}{L}, \omega) = \frac{-2P_I \sum_{m=-\infty}^{\infty} Y(k_x + \frac{2\pi m}{L}, \omega)}{1 - \frac{M\omega^2}{L} \sum_{m=-\infty}^{\infty} Y(k_x + \frac{2\pi m}{L}, \omega)}. \tag{45}$$

Inserting equation (45) into equation (38) yields

$$U_z(k_x, \omega) = -2P_I Y(k_x, \omega) + \frac{M\omega^2}{L} \left[\frac{-2P_I \sum_{m=-\infty}^{\infty} Y(k_x + \frac{2\pi m}{L}, \omega)}{1 - \frac{M\omega^2}{L} \sum_{m=-\infty}^{\infty} Y(k_x + \frac{2\pi m}{L}, \omega)} \right] Y(k_x, \omega). \tag{46}$$

After some rearrangement, the displacement of the system becomes

$$\frac{U_z(k_x, \omega)}{P_I} = -2Y(k_x, \omega) \left[\frac{1}{1 - \frac{M\omega^2}{L} \sum_{m=-\infty}^{\infty} Y(k_x + \frac{2\pi\, m}{L}, \omega)} \right], \tag{47}$$

or

$$\frac{U_z(k_x,\omega)}{P_I} = -2\left(Dk_x^4 - \rho h\omega^2 + \frac{\rho_f\omega^2}{i\gamma}\right)^{-1}\left\{1 - \frac{M\omega^2}{L}\sum_{m=-\infty}^{\infty}\left[\frac{1}{D\left(k_x + \frac{2\pi m}{L}\right)^4 - \rho h\omega^2 + \frac{\rho_f\omega^2}{i\gamma}}\right]\right\}^{-1} \quad (48)$$

Equation (48) is the displacement of the system with periodic masses. Note that when $M = 0$ or $L \to \infty$, the expression is identical to equation (5), and when $M \to \infty$, the limit of the expression is equal to zero.

Two different example problems are now computed for the thin plate response with periodic masses. Figure 26 is an image of thin plate normalized velocity versus wavenumber and frequency generated using equations (28) and (48) for $M = 1.0$ kg/m and $L = 0.01$ meter. Figure 27 is an image of thin plate normalized velocity versus wavenumber and frequency generated using equations (28) and (48) for $M = 4.0$ kg/m and $L = 0.01$ meter. Figures 28 through 31 are constant frequency cuts of figures 2, 26, and 27 overlaid for a frequency range of 1.0–4.0 kHz in 1.0-kHz increments. (Figures 28 through 31 display velocity on a decibel scale.)

Normal Velocity (dB) - Thin Plate Model
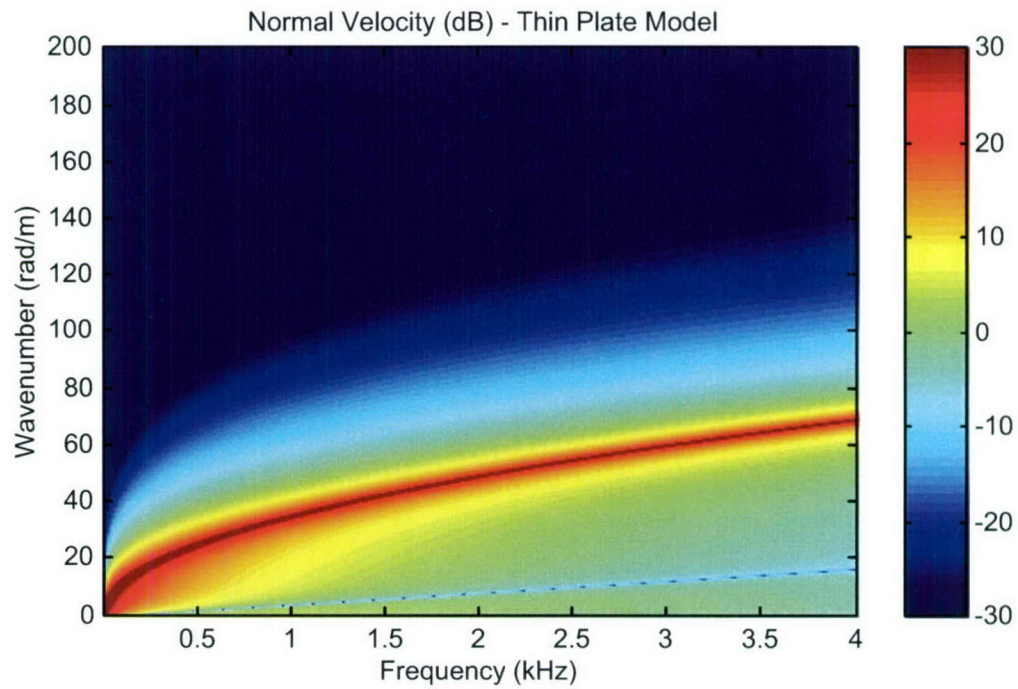
Figure 26. Normalized Velocity Versus Wavenumber and Frequency at M = 1.0 kg/m and L = 0.01 m—Modeled Using Thin Plate Theory

Normal Velocity (dB) - Thin Plate Model
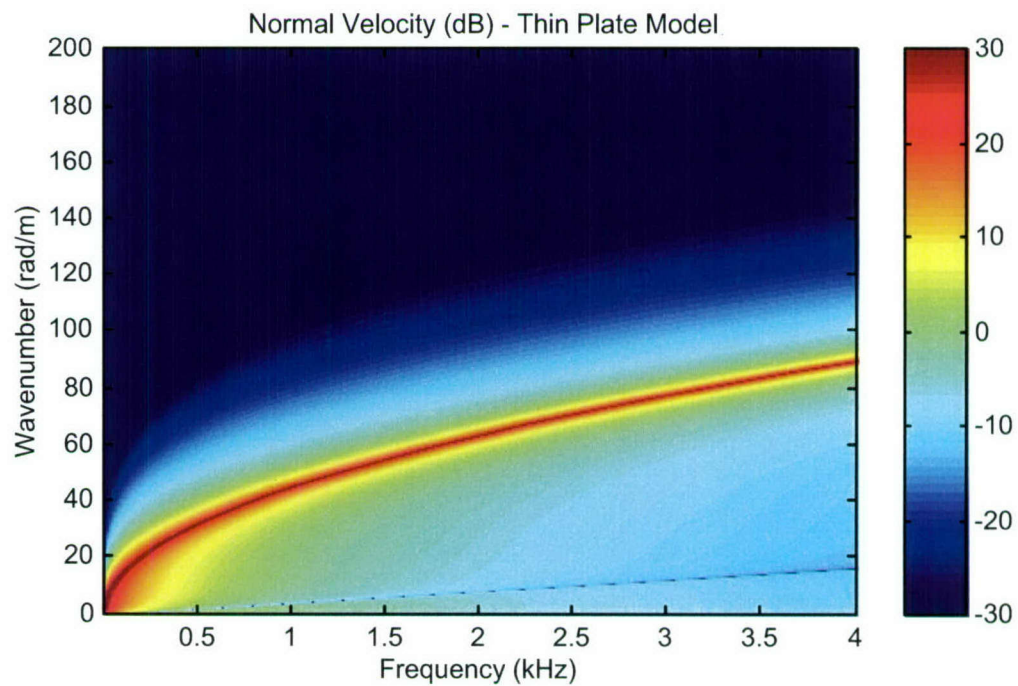
Figure 27. Normalized Velocity Versus Wavenumber and Frequency at M = 4.0 kg/m and L = 0.01 m—Modeled Using Thin Plate Theory
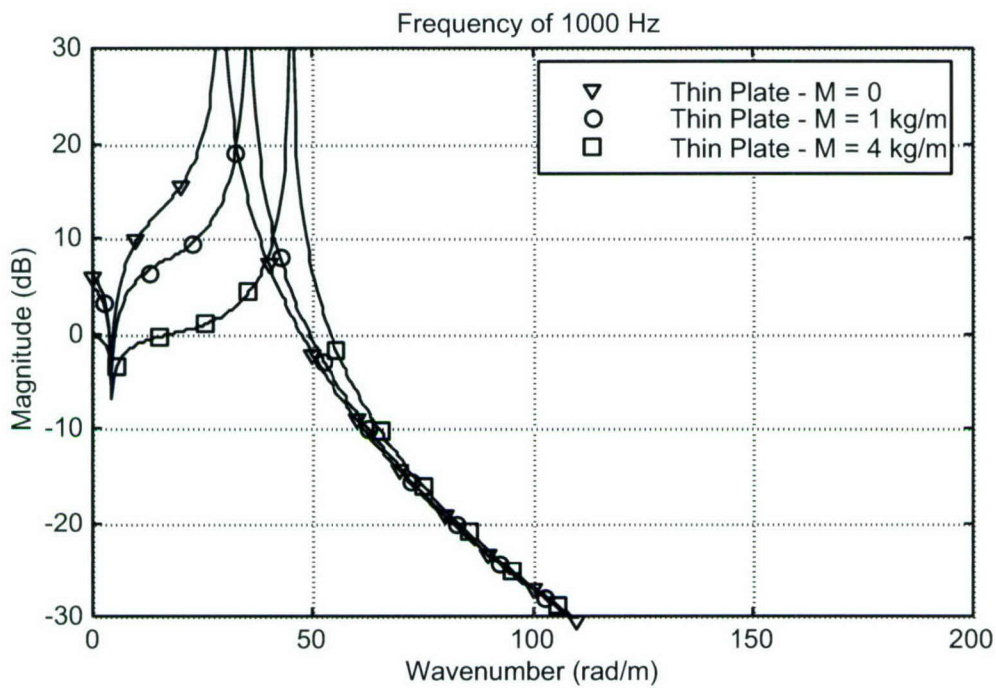
Figure 28. Normalized Velocity Versus Wavenumber—Modeled Using Thin Plate Theory with Masses at 1.0 kHz
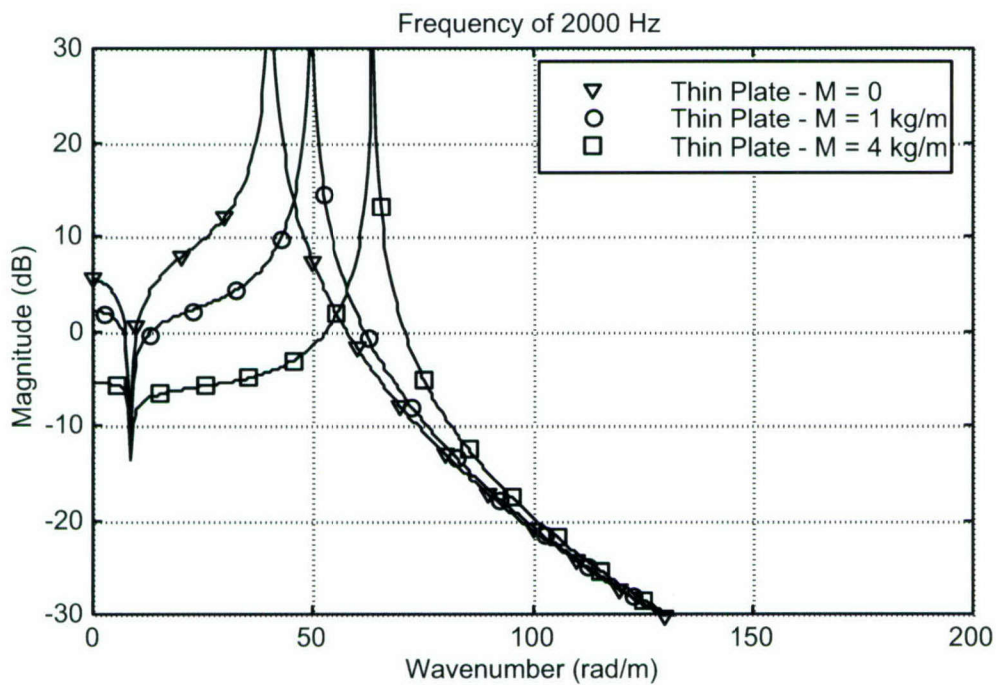
Figure 29. Normalized Velocity Versus Wavenumber—Modeled Using Thin Plate Theory with Masses at 2.0 kHz

27

Figure 30. Normalized Velocity Versus Wavenumber—Modeled Using Thin Plate Theory with Masses at 3.0 kHz

Figure 31. Normalized Velocity Versus Wavenumber—Modeled Using Thin Plate Theory with Masses at 4.0 kHz

3.2. TIMOSHENKO-MINDLIN PLATE WITH MASSES

The second model investigated is that of a thin plate with rotary inertia and shear containing the periodic masses with a fluid load on top. The equation of motion of this system is

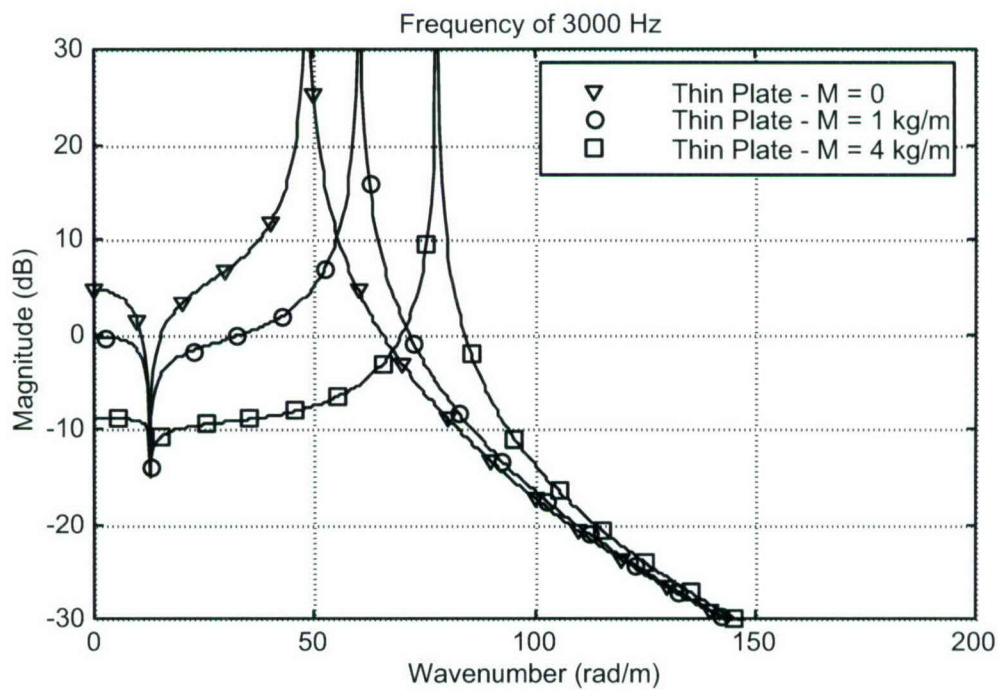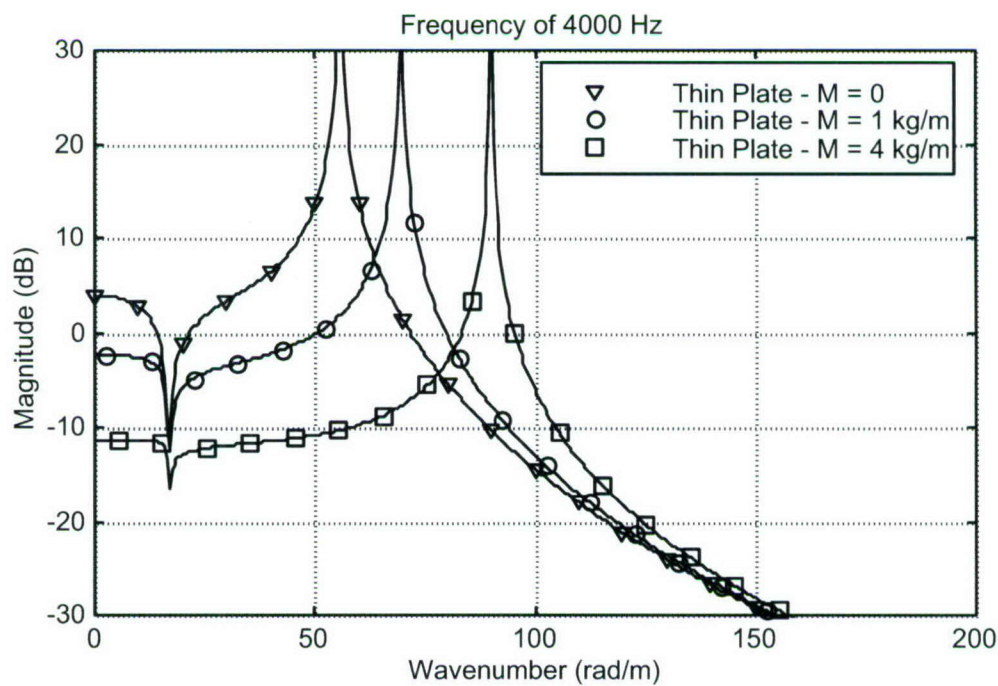$$D\frac{\partial^4 u_z(x,t)}{\partial x^4} - \left(\frac{D\rho}{\kappa G} + \frac{\rho h^3}{12}\right)\frac{\partial^4 u_z(x,t)}{\partial x^2 \partial t^2} + \left(\frac{\rho^2 h^3}{12\kappa G}\right)\frac{\partial^4 u_z(x,t)}{\partial t^4} + \rho h\frac{\partial^2 u_z(x,t)}{\partial t^2}$$

$$= -p(x,t) + \left(\frac{D}{\kappa Gh}\right)\frac{\partial^2 p(x,t)}{\partial x^2} - \left(\frac{\rho h^2}{12\kappa G}\right)\frac{\partial^2 p(x,t)}{\partial t^2} - p_M(x,t), \qquad (49)$$

where the interaction of the fluid and the plate contains rotary inertia and shear effects, and the interaction of the discrete masses with the plate does not contain rotary inertia or shear effects. This assumption has been included to greatly simplify the model. As with the thin plate, the displacement can be determined by

$$\frac{U_z(k_x,\omega)}{P_I} = -2Z(k_x,\omega)\left[\frac{1}{1 - \dfrac{M\omega^2}{L}\displaystyle\sum_{m=-\infty}^{\infty} Z\left(k_x + \dfrac{2\pi m}{L},\omega\right)}\right], \qquad (50)$$

where

$$Z(k_x,\omega) = \frac{1 + \left(\dfrac{D}{\kappa Gh}\right)k_x^2 - \left(\dfrac{\rho h^2}{12\kappa G}\right)\omega^2}{Dk_x^4 + \left(\dfrac{D\rho_f}{i\gamma\kappa Gh} - \dfrac{D\rho}{\kappa G} - \dfrac{\rho h^3}{12}\right)\omega^2 k_x^2 + \left(\dfrac{\rho^2 h^3}{12\kappa G} - \dfrac{\rho_f \rho h^2}{12 i\gamma\kappa G}\right)\omega^4 + \left(\dfrac{\rho_f}{i\gamma} - \rho h\right)\omega^2}. \qquad (50)$$

Note that when $M = 0$ or $L \to \infty$, the expression is identical to equation (9); when $M \to \infty$, the limit of the expression is equal to zero.

29

The two example problems that were computed for the thin plate response with periodic masses are now repeated for the thin plate with rotary inertia and shear effects. Figure 32 is an image of Timoshenko-Mindlin plate normalized velocity versus wavenumber and frequency generated using equations (28) and (50) for $M = 1.0$ kg/m and $L = 0.01$ meter. Figure 33 is an image of Timoshenko-Mindlin plate normalized velocity versus wavenumber and frequency generated using equations (28) and (50) for $M = 4.0$ kg/m and $L = 0.01$ meter. Figures 34 through 37 are constant frequency cuts of figures 3, 32, and 33 overlaid for a frequency range of 1.0-4.0 kHz in 1.0-kHz increments. (Figures 34 through 37 display velocity in a decibel scale.)

Normal Velocity (dB) - Timoshenko-Mindlin Plate Model

Figure 32. Normalized Velocity Versus Wavenumber and Frequency at M = 1.0 kg/m and L = 0.01 m—Modeled Using Timoshenko-Mindlin Plate Theory

Normal Velocity (dB) - Timoshenko-Mindlin Plate Model

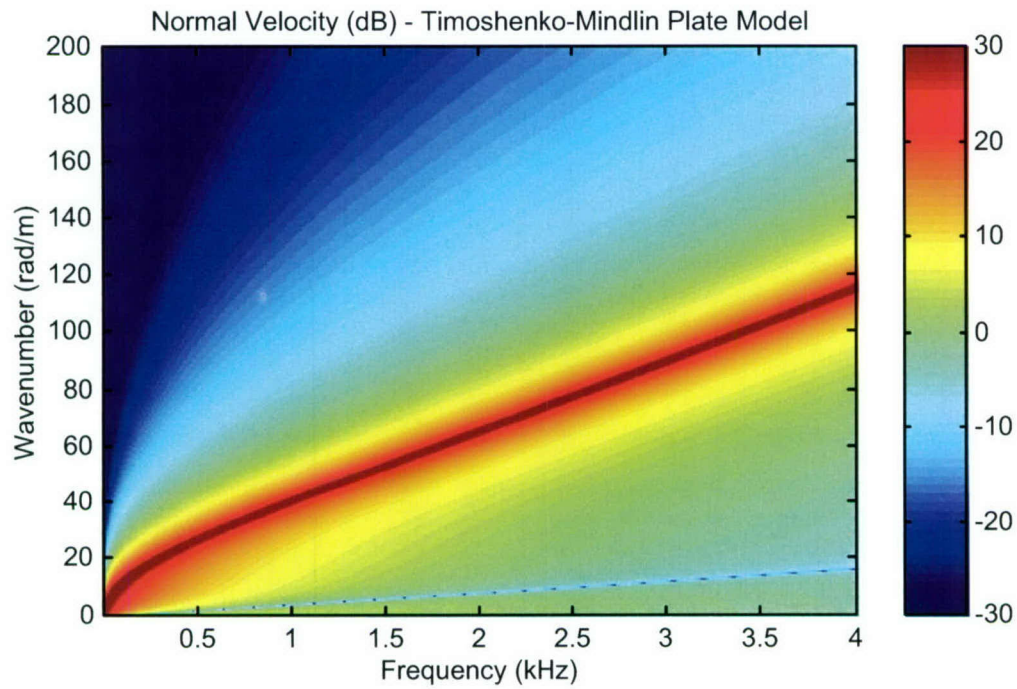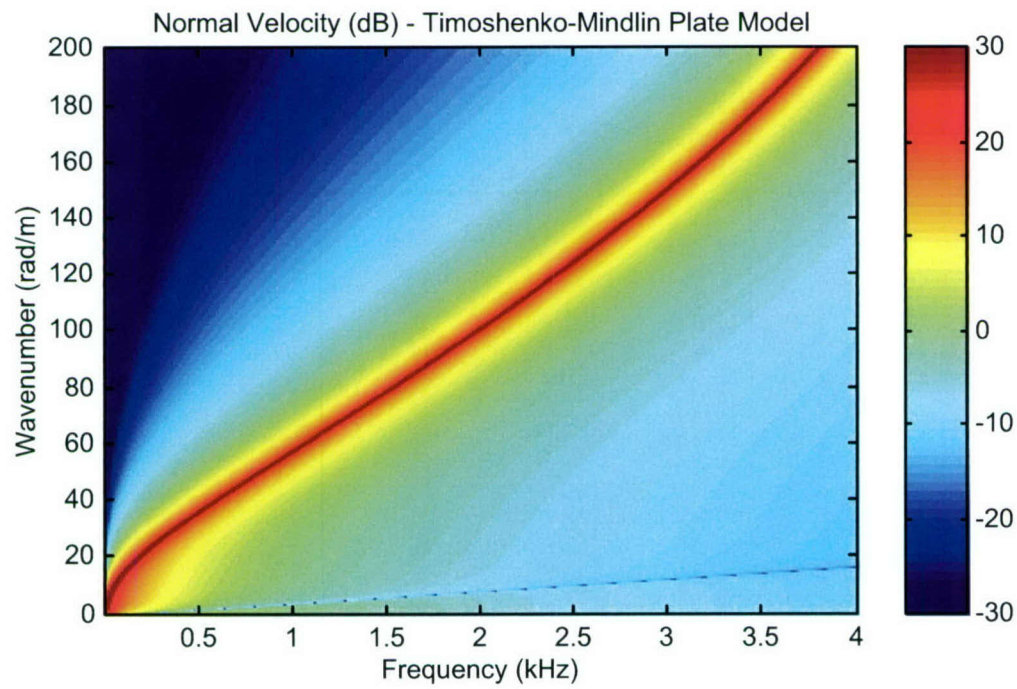**Figure 33. Normalized Velocity Versus Wavenumber and Frequency at M = 4.0 kg/m and L = 0.01 m—Modeled Using Timoshenko-Mindlin Plate Theory**

Figure 34. Normalized Velocity Versus Wavenumber—Modeled Using Timoshenko-Mindlin Plate Theory with Masses at 1.0 kHz

Figure 35. Normalized Velocity Versus Wavenumber—Modeled Using Timoshenko-Mindlin Plate Theory with Masses at 2.0 kHz

Frequency of 3000 Hz

Figure 36. Normalized Velocity Versus Wavenumber—Modeled Using Timoshenko-Mindlin Plate Theory with Masses at 3.0 kHz

Frequency of 4000 Hz

Figure 37. Normalized Velocity Versus Wavenumber—Modeled Using Timoshenko-Mindlin Plate Theory with Masses at 4.0 kHz

33

3.3. THICK PLATE WITH MASSES

Thick plate theory is now investigated using the finite-element method. The problem of added mass with $L = 0.01$ meter and $M = 4.0$ kg/m is modeled using SARAH2D, a commercial finite-element program.[14] Initially, the plate is modeled without masses and compared to the results from equation (11). Figure 38 shows the finite-element analysis results for the fluid-loaded plate without the masses, and figure 39 shows the same results using thick plate theory. Note that these two figures are nearly identical except for grid discretization. Figure 40 is the finite-element results for the fluid-loaded thick plate with $L = 0.01$ meter and $M = 4.0$ kg/m. Figure 41 shows cuts of figures 38 and 40 at 0° and 30°, which correspond to an apparent wave speeds of infinity and 3000 m/s, respectively. Notice that the major effects of the periodic masses are at lower frequencies. Finally, figure 42 shows cuts of figures 38 and 40 at 100 and 150 rad/m. The masses have a large effect on the dynamics of the system at low frequency and low wavenumber—they have very little impact on the response of the system at high frequency.
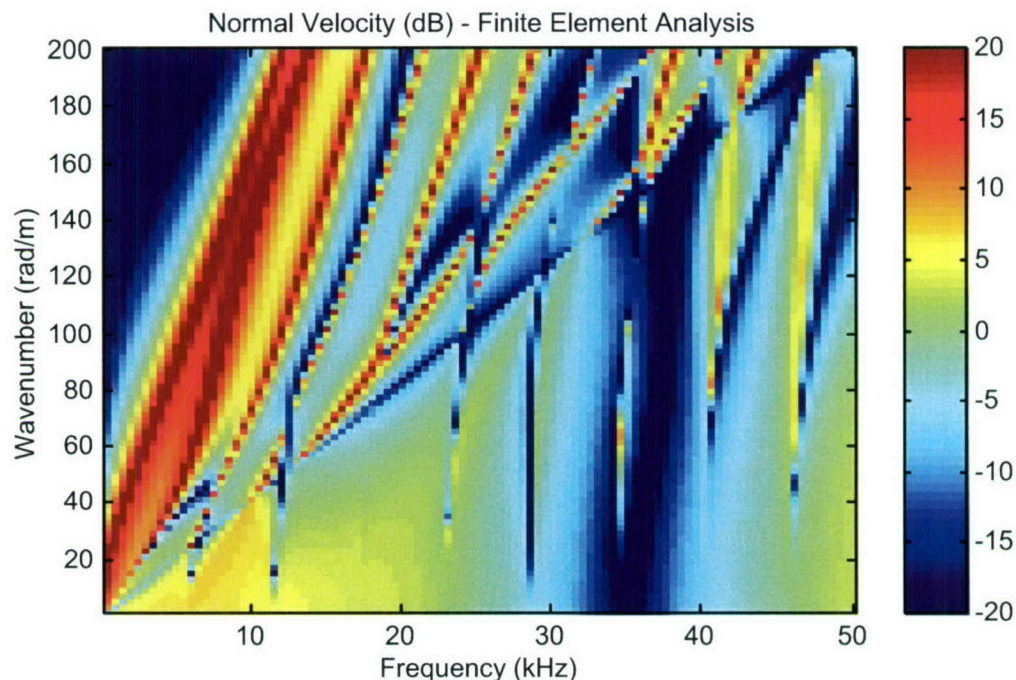
Figure 38. Normalized Velocity Versus Wavenumber and Frequency Without Mass—Modeled Using Finite-Element Theory

Normal Velocity (dB) - Thick Plate Model
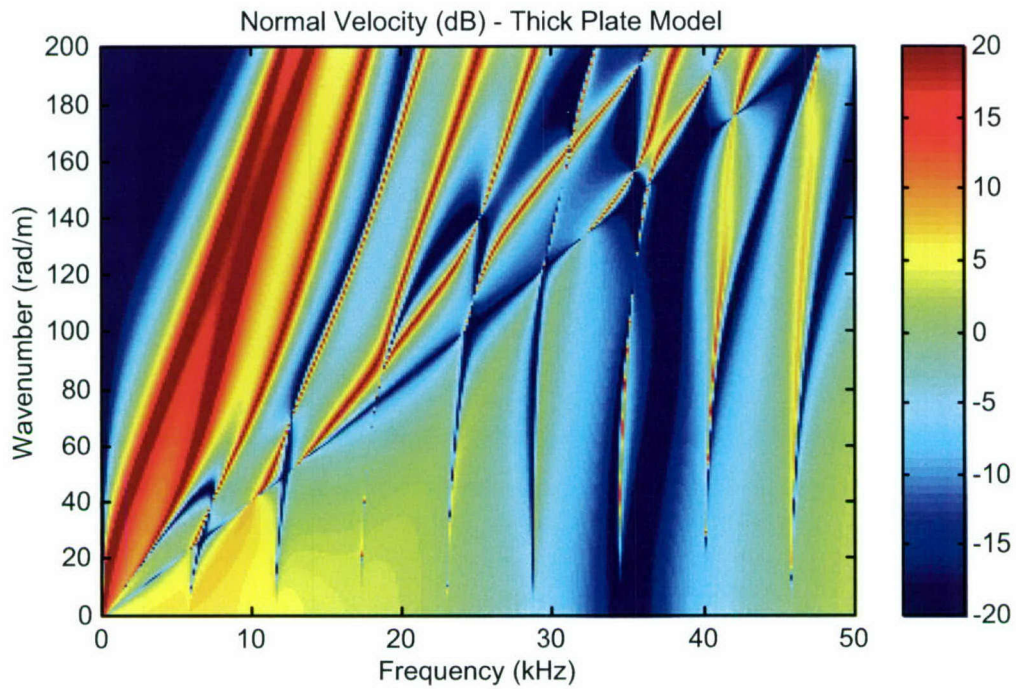
Figure 39. Normalized Velocity Versus Wavenumber and Frequency Without Mass—Modeled Using Thick Plate Theory

Normal Velocity (dB) - Finite Element Analysis

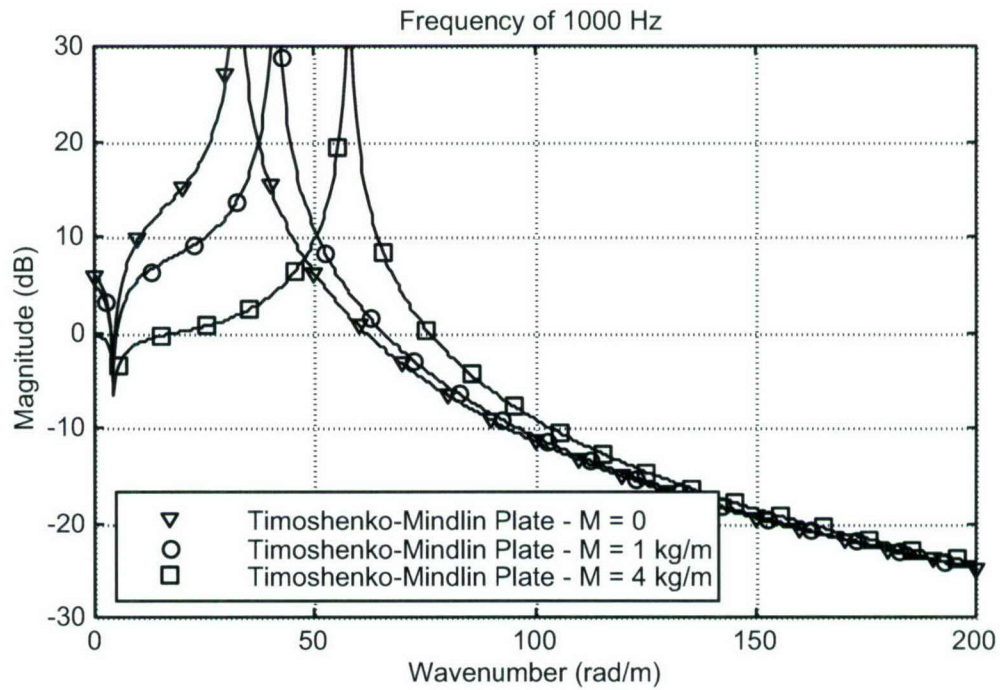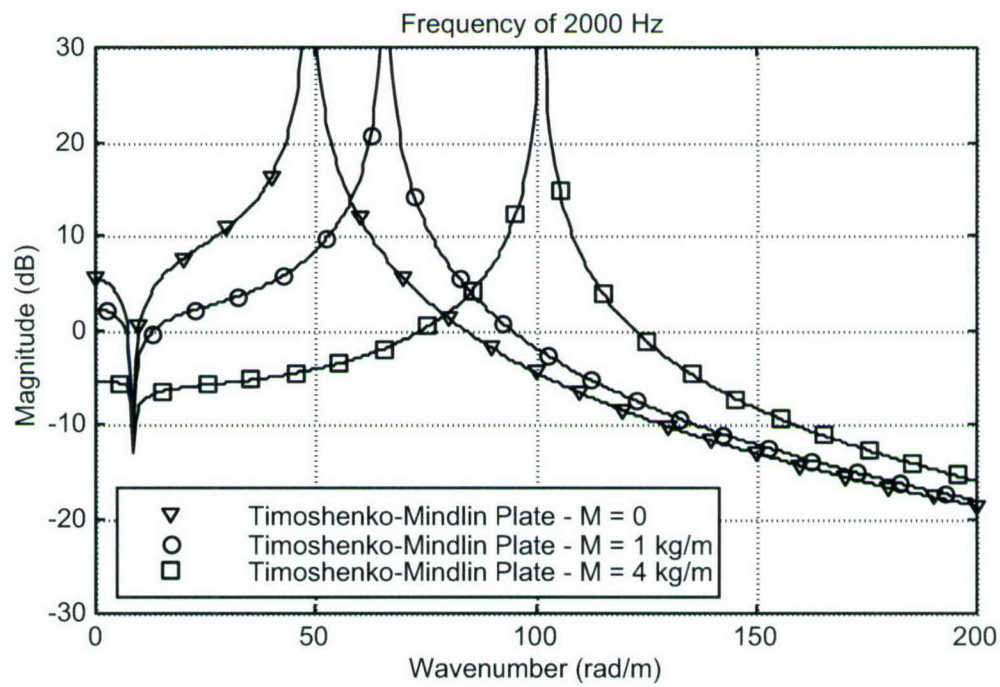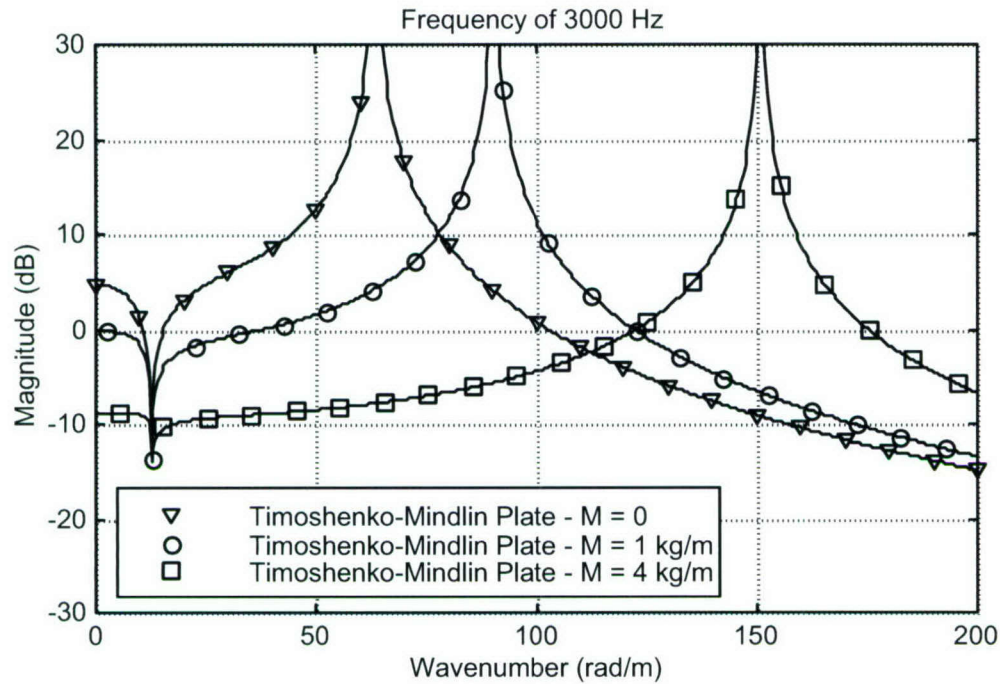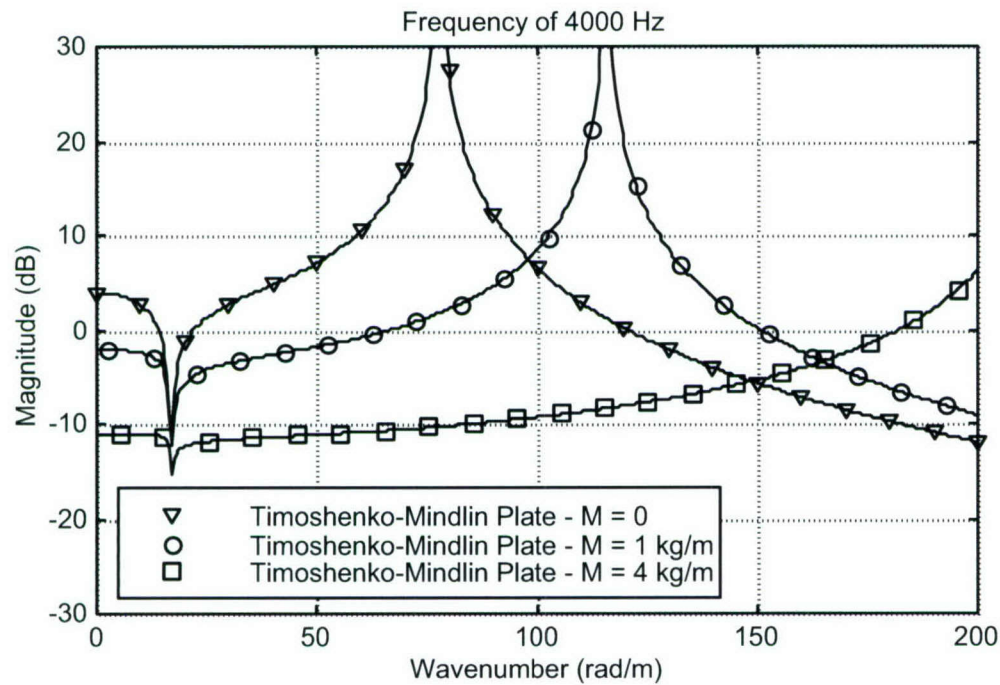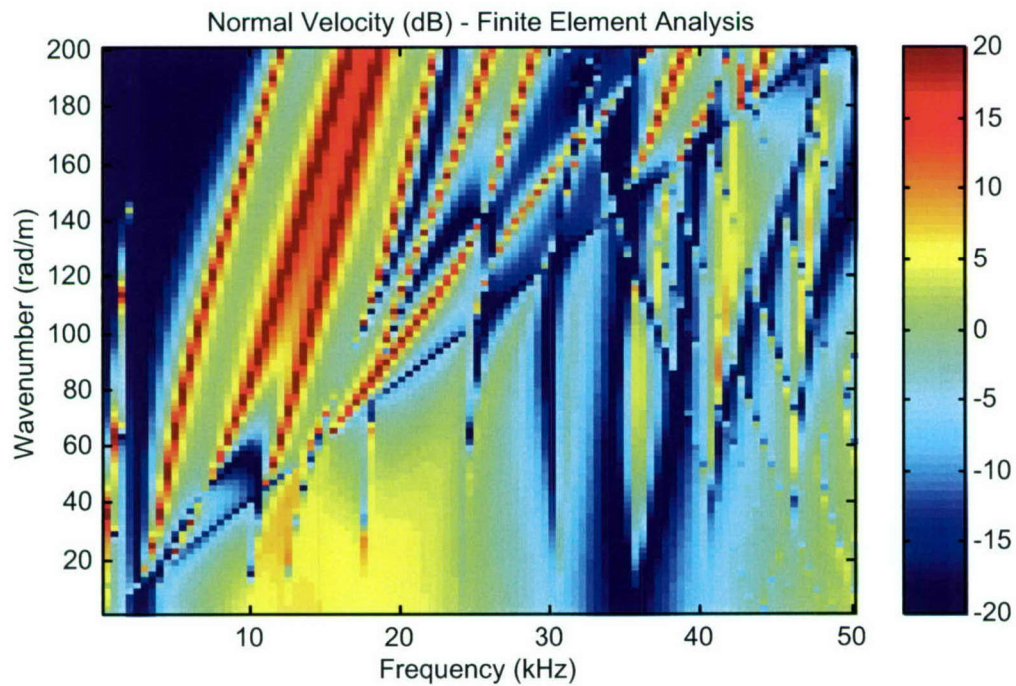*Figure 40. Normalized Velocity Versus Wavenumber and Frequency with M = 4.0 kg/m and L = 0.01 m—Modeled Using Finite-Element Theory*

35

Normal Velocity (dB) - Cut at 0 degrees

Normal Velocity (dB) - Cut at 30 degrees

Figure 41. Normalized Velocity Versus Frequency—Modeled
Using Finite-Element Theory, Cuts at 0° and 30°

36

***Figure 42. Normalized Velocity Versus Frequency—Modeled
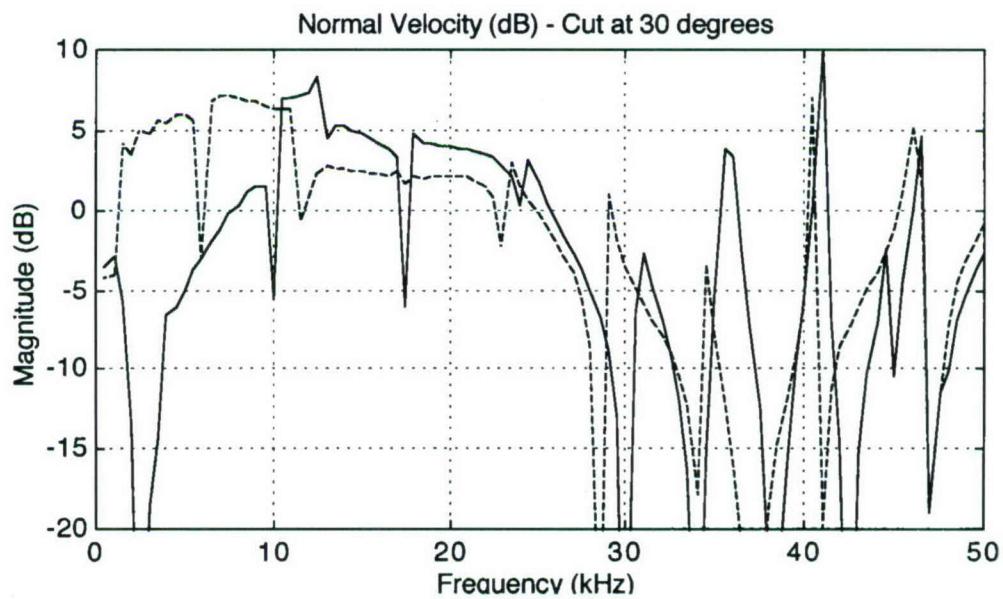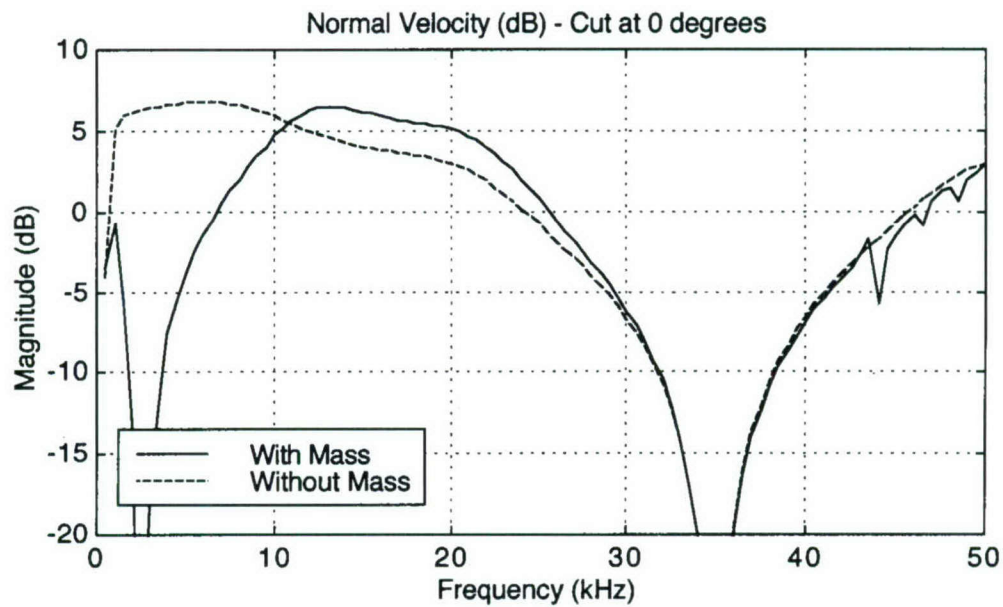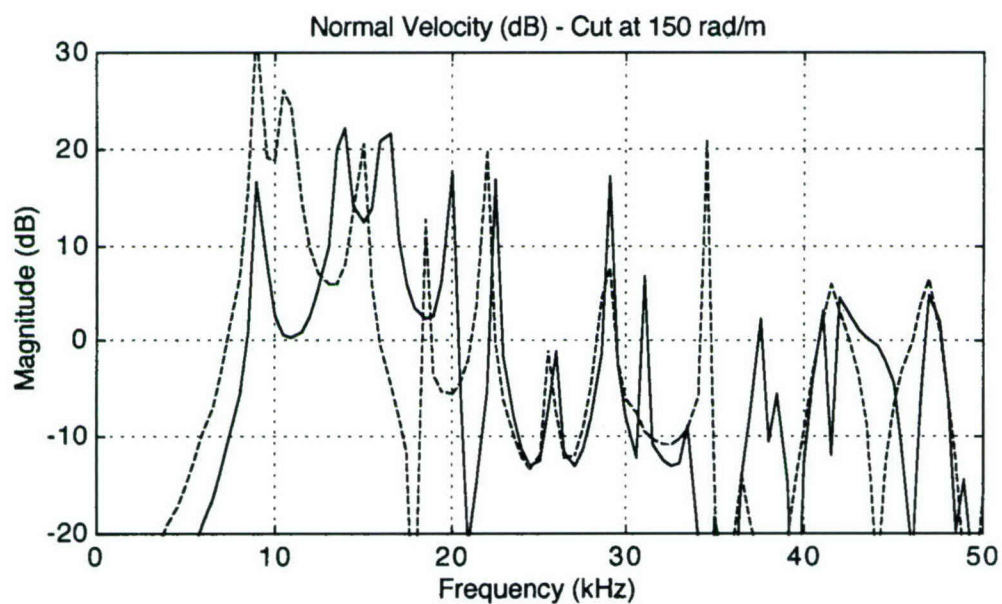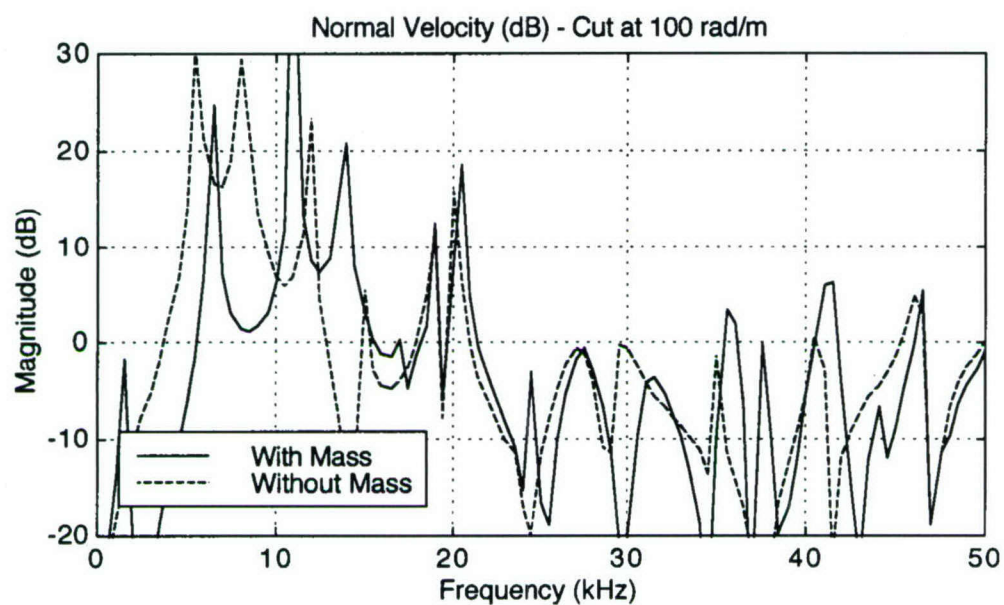Using Finite-Element Theory, Cuts at 100 rad/m and 150 rad/m***

4. ELASTICITY EQUATIONS OF MOTION

The derivation of the fully elastic equations of motion are presented below. An earlier report[7] derived the following stress relationships at the surface of the plate for normal and tangential stress, respectively:

$$\tau_{zz}(x,b,t) = (\lambda + 2\mu)\frac{\partial u_z(x,b,t)}{\partial z} + \lambda \frac{\partial u_x(x,b,t)}{\partial x} = - p_1(x,b,t), \tag{52}$$

and

$$\tau_{zx}(x,b,t) = \mu\left[\frac{\partial u_x(x,b,t)}{\partial z} + \frac{\partial u_z(x,b,t)}{\partial x}\right] = 0. \tag{53}$$

The stress relationships at the bottom of the plate are

$$\tau_{zz}(x,a,t) = (\lambda + 2\mu)\frac{\partial u_z(x,a,t)}{\partial z} + \lambda \frac{\partial u_x(x,a,t)}{\partial x} = 0, \tag{54}$$

and

$$\tau_{zx}(x,a,t) = \mu\left[\frac{\partial u_x(x,a,t)}{\partial z} + \frac{\partial u_z(x,a,t)}{\partial x}\right] = 0. \tag{55}$$

If the mass is on the bottom surface of the plate, equations (54) and (55) are modified to become

$$\tau_{zz}(x,a,t) = (\lambda + 2\mu)\frac{\partial u_z(x,a,t)}{\partial z} + \lambda \frac{\partial u_x(x,a,t)}{\partial x} = M \sum_{n=-\infty}^{\infty} \frac{\partial u_z(x,t)}{\partial t^2}\delta(x - nL), \tag{56}$$

and

$$\tau_{zx}(x,a,t) = \mu\left[\frac{\partial u_x(x,a,t)}{\partial z} + \frac{\partial u_z(x,a,t)}{\partial x}\right] = M \sum_{n=-\infty}^{\infty} \frac{\partial u_x(x,t)}{\partial t^2}\delta(x - nL). \tag{57}$$

The displacements of the system are

$$u_x(x,z,t) = U_x(k_x,z,\omega)\exp(ik_x x)\exp(i\omega t)$$

$$= \left[A(k_x,\omega)ik_x \exp(i\alpha z) + B(k_x,\omega)ik_x \exp(-i\alpha z) \right.$$

$$\left. - C(k_x,\omega)i\beta \exp(i\beta z) + D(k_x,\omega)i\beta \exp(-i\beta z) \right]\exp(ik_x x)\exp(i\omega t), \qquad (58)$$

and

$$u_z(x,z,t) = U_z(k_x,z,\omega)\exp(ik_x x)\exp(i\omega t)$$

$$= \left[A(k_x,\omega)i\alpha \exp(i\alpha z) - B(k_x,\omega)i\alpha \exp(-i\alpha z) \right.$$

$$\left. + C(k_x,\omega)ik_x \exp(i\beta z) + D(k_x,\omega)ik_x \exp(-i\beta z) \right]\exp(ik_x x)\exp(i\omega t). \qquad (59)$$

To obtain a solution, equations (58) and (59) are inserted into equations (52), (53), (56), and (57) and the coefficients A, B, C, and D need to be determined. As posed, it is unclear if this solution exists.

5. CONCLUSIONS

This report has derived the quations of motion of a fluid-loaded thin plate that contains embedded masses when it is forced by an acoustic plane wave at a specific wavenumber. The equations were copled to the fluid and the masses and then manipulated to determine the displacement field. The method was then applied to a Timoshenko-Mindlin plate and to a thick plate.

Several conclusions were supported by this study. For a soft elastomeric-type material with thickness of 0.04 meter or less, thin plate equations of motion are valid to about 1.5 kHz, and Timoshenko-Mindlin plate equations of motion are valid to around 3.5 kHz. These results are independent of periodic masses. The problem of periodic masses in a thin plate and in a Timoshenko-Mindlin plate with a fluid load on the top and a plane acoustic wave excitation have been derived and analyzed using different size masses. The problem of periodic masses in a thick plate with a fluid load on the top and a plane acoustic wave excitation has been analyzed using finite element methods for one size mass. The problem has also been formulated using thick plate equations of motion.

It is recommended that the thick shell equations of motion be modified to handle the periodic masses and examined to determine if a closed-form solution exists.

6. REFERENCES

1. A. Leissa, *Vibration of Plates*, American Institute of Physics, College Park, MD, 1973.

2. H. Lamb, "On Waves in an Elastic Plate," *Proceedings of the Royal Society of London, Series A*, vol. 93, 1917, pp. 114-120.

3. A. Freedman, "The Variation, with the Poisson Ratio, of Lamb Modes in a Free Plate, I: General Spectra," *Journal of Sound and Vibration*, vol. 137, no. 2, 1990, pp. 209-230.

4. M. F. M. Osborne and S. D. Hart, "Transmission, Reflection, and Guiding of an Exponential Pulse by a Steel Plate in Water, I: Theory," *Journal of the Acoustical Society of America*, vol. 17, no. 1, 1945, pp. 1-18.

5. D. G. Crighton, "The Free and Forced Waves on a Fluid-Loaded Elastic Plate," *Journal of Sound and Vibration*, vol. 63, no. 2, 1979, pp. 225-235.

6. J. H. Su and R. Vasudevan, "On the Radiation Efficiency of Infinite Plates Subjected to a Point Load in Water," *Journal of Sound and Vibration*, vol. 208, no. 3, 1997, pp. 441-455.

7. A. J. Hull, "Analysis of a Fluid-Loaded Thick Plate," NUWC-NPT Technical Report 11,389, Naval Undersea Warfare Center Division, Newport, RI, 1 October 2002.

8. V. N. Romanov, "Radiation of Sound by an Infinite Plate with Reinforcing Beams," *Soviet Physics-Acoustics*, vol. 17, 1971, pp. 92-96.

9. B. R. Mace, "Sound Radiation from a Plate Reinforced by Two Sets of Parallel Stiffeners," *Journal of Sound and Vibration*, vol. 71, no. 3, 1981, pp. 435-441.

10. B. A. Cray, "Acoustic Radiation from Periodic and Sectionally Aperiodic Rib-Stiffened Plates," *Journal of the Acoustical Society of America*, vol. 95, no. 1, 1994, pp. 256-264.

11. A. J. Hull, "Derivation of Transfer Functions for a Fluid-Loaded, Multiple-Layer Thick Plate System," NUWC-NPT Technical Report 11,245, Naval Undersea Warfare Center Division, Newport, RI, 15 September 2000.

12. K. F. Graff, *Wave Motion in Elastic Solids*, Dover Publications, New York, 1975.

13. S. P. Timoshenko and J. N. Goodier, *Theory of Elasticity*, McGraw-Hill, New York, 1934.

14. Private communication with S. A. Hassan, Naval Undersea Warfare Center Division, Newport, RI, 2004.

INITIAL DISTRIBUTION LIST

Addressee	No. of Copies
Office of Naval Research (ONR 333: D. Drumheller, K. Ng)	2
Defense Technical Information Center	2
Center for Naval Analyses	1